



Cite this: *Lab Chip*, 2017, 17, 3960

Received 16th June 2017,
Accepted 7th September 2017

DOI: 10.1039/c7lc00627f

rsc.li/loc

Why microfluidics? Merits and trends in chemical synthesis

Yong Liu^{ab} and Xingyu Jiang ^{*ab}

The intrinsic limitations of conventional batch synthesis have hindered its applications in both solving classical problems and exploiting new frontiers. Microfluidic technology offers a new platform for chemical synthesis toward either molecules or materials, which has promoted the progress of diverse fields such as organic chemistry, materials science, and biomedicine. In this review, we focus on the improved performance of microreactors in handling various situations, and outline the trend of microfluidic synthesis (microsynthesis, μ Syn) from simple microreactors to integrated microsystems. Examples of synthesizing both chemical compounds and micro/nanomaterials show the flexible applications of this approach. We aim to provide strategic guidance for the rational design, fabrication, and integration of microdevices for synthetic use. We critically evaluate the existing challenges and future opportunities associated with this burgeoning field.

1 Introduction

Synthetic chemistry, one of the oldest scientific subjects, plays a key role in promoting the progress of human society. However, the intrinsic limitations of conventional batch synthesis have long prevented it from solving problems both classical and new. For instance, the poor selectivity of batch reactors explains their mediocre performance in obtaining desired products with controllable structures and properties,

such as modifying molecules at the specific site or tuning the layered structure of micro/nanomaterials.^{1,2} Moreover, their low level of integration and automation severely hampers their application in combinatorial synthesis, screening, and optimization.³ Other issues mainly include (i) complex stepwise operation, (ii) waste of resources (e.g., time, reagent, equipment, and labor), (iii) poor reproducibility, and (iv) safety concerns, which make batch methods anything but green and smart (Fig. 1A).⁴

These disadvantages result in an adverse knock-on effect on diverse research fields ranging from materials science to biomedicine. For instance, stepwise preparation of hybrid nanoparticles (e.g., core-shell structures) in batch reactors by either a top-down or bottom-up approach is time-consuming, and has poor size distribution with large batch-to-batch

^a Beijing Engineering Research Center for BioNanotechnology & CAS Key Laboratory for Biological Effects of Nanomaterials and Nanosafety, CAS Center for Excellence in Nanoscience, National Center for Nanoscience and Technology, Beijing 100190, P. R. China. E-mail: xingyujiang@nanoctr.cn

^b University of Chinese Academy of Sciences, Beijing 100049, P. R. China



Yong Liu obtained his B.S. at Wuhan University (2016, Chemistry). He is currently a Ph.D. candidate at the National Center for Nanoscience and Technology (NCNST) under the supervision of Prof. Xingyu Jiang. His current scientific interest is focused on microfluidics-assisted biochemical analysis and materials synthesis.

Yong Liu



Xingyu Jiang obtained his B.S. at the University of Chicago (1999), followed by an A.M. (2001) and a Ph.D. (2004) from Harvard University (Chemistry), working with Prof. George Whitesides. He joined the NCNST in 2005 where he has remained since. Xingyu's research interests include surface chemistry and microfluidics.

Xingyu Jiang

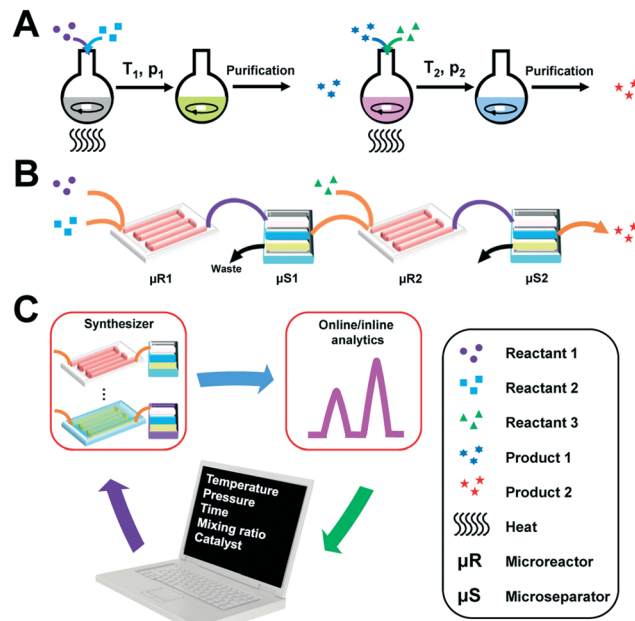


Fig. 1 Conceptual framework of different synthetic methods using a traditional two-step process as an example. (A) Batch synthesis with beakers and flasks in a step-by-step manner with two individual purification steps. (B) Multistage flow synthesis in a continuous manner with two microreactors for reaction and two microseparators for purification. (C) An automated and integrated microsystem with different functional modules: the microsynthesizer for product formation, the online/inline detector for product detection, and a computer for control and optimization of many variables such as the temperature and the mixing ratio.

variation, which shows a negative impact on their functionalities as sensing probes or reagent carriers.⁵ Besides, drug/material discovery in batch reactors is rather inefficient with low throughput and long cycle time, which greatly encumbers the development of novel tools for biosensing, cancer therapeutics, and tissue engineering.⁶ These drawbacks also prevent batch methods from intersecting with some burgeoning areas that can benefit the current state of synthetic chemistry, such as green synthesis, big data, chemo/bioinformatics, and precision biomedicine.

Microfluidic technology that originates as a technique modulating fluids in microscale channels has found broad applications in biochemical engineering,^{7–9} which is exemplified by the multiplexed detection of biomarkers and the precise manipulation of cell behaviors, from the individual to the collective.^{10,11} The past few decades have witnessed the emergence and explosion of microfluidic platforms as alternative routes of chemical synthesis toward both molecules and materials.^{12,13} Microfluidics has two major advantages for synthesis: (i) mixing and heat/mass transfer in short time/space scales; (ii) precise control down to nm and pL levels. Unlike batch methods, μ Syn typically proceeds in the flowing liquid confined by miniaturized microreactors such as microtubes, microchannels, microdroplets, microinterfaces, microcapsules, and even biological cells (Fig. 1B).^{14–19} The facility

of microreactor design and fabrication extends its applicability in various situations with improved efficiency, controllability, and safety, which has been demonstrated in a range of applications.^{20–24}

Despite the great success in preparing different products, a simple/single microreactor suffers from several limitations: (i) low throughput for either screening or production; (ii) offline analysis requiring external instruments; (iii) complex manual intervention involved especially for optimization and decision making. Tackling these problems requires the integration of microreactors in two aspects: (i) internal integration toward improved throughput to conduct multiple processes in parallel;^{25–28} (ii) external integration with other functional modules such as automatics, online/inline analytics, and feedback devices (Fig. 1C).^{29–31} These concepts have inspired the recent development of highly integrated and fully automated microsystems, with exciting results in materials screening and self-optimization of continuous/discrete reaction variables.^{32–34} Scale-up of microreactors toward high productivity/stability helps to bridge the gap between academia and clinical/industrial translation.^{35–39} The existing challenges of batch synthesis and possible solutions from microfluidics are summarized in Table 1.

From concept to practice, μ Syn has brought tremendous changes to synthetic chemistry and relevant fields, opening up new routes toward the desired product while offering an insight into the mechanism at the molecular level.^{40–42} It inspires a boom/trend to apply microfluidics in either studying classical synthesis or developing novel molecules/materials, which has promoted the development of organic chemistry, materials science, and biomedicine. Moreover, microfluidics offers a simple but ideal interface to connect synthetic chemistry with several emerging technologies that are leading worldwide revolution, such as three-dimensional (3D) printing, big data, and artificial intelligence.^{43–45} μ Syn is becoming an interdisciplinary science with both challenges and opportunities for researchers to exploit endless possibilities.

Existing reviews on similar topics artificially break the landscape of μ Syn into two separate aspects, compounds and materials, and focus on either of them, failing to provide the readers with a comprehensive overview of the promising field. They are largely limited to simple microreactor-assisted synthesis with only a few groups conceptually, but not sufficiently, sketching the recent advances of integrated and smart microsynthesizers. However, to overcome these limitations, we organize this review based on the design principles of microfluidic synthesizers to achieve improved performance in several specific situations, from micromixing to large-scale synthesis. We illustrate the common basics that work in obtaining both small molecules and micro/nanomaterials and, meanwhile, outline the unstoppable trend of μ Syn toward integration and intelligence. Finally, we evaluate the current challenges and future possibilities of microfluidics-assisted chemical synthesis.

Table 1 How could microfluidics help with synthetic chemistry?

	Existing challenges	Microfluidic solutions	Example
Operation	Stepwise and manual operation, waste of time, reagents, and labor, poor reproducibility Safety concerns, hazards, <i>e.g.</i> , heat, pressure, and toxic chemicals	Continuous synthesis, short residence time, minimal reagent consumption, automation	Ref. 20–22 and 29
Regulation	Poor control of reaction parameters and environments	Tight control of reaction parameters and reagent delivery, rapid mixing and heat/mass transfer, no need to store the intermediates, low exposure to hazards	Ref. 24, 69 and 105
Integration	Poor product selectivity External instruments required for product detection Low screening/optimization efficiency	Small size, flexible design, precise control/manipulation of the flow, <i>e.g.</i> , temperature, pressure, flow path, flow rate, residence time, and reagent transport scheme Online/inline analytics for real-time monitoring High-throughput chips, automation, program control, self-optimization	Ref. 23, 40, 49, 53, 71 and 93 Ref. 41 and 126–134 Ref. 25–28 and 32–34

2 Microfluidics and micromixing

Over the centuries, we have run synthetic chemistry in beakers and flasks simply because their sizes perfectly suit our hands. An interesting question thus arises, however, from a synthetic perspective, will molecules feel comfortable in a macroscale container? Our answer is definitely no! At the molecular level, a reaction occurs when two molecules collide with each other, which, in macroscopic view, we refer to as the mixing of reactants. It often takes minutes to reach a homogeneous solution in batch reactors by stirring, which greatly exceeds the lifetime of molecular collision (<ps), and can cause adverse consequences such as intense heat release and reduction of yield, especially for processes with fast kinetics.

Mixing in microfluids is different from that in bulk solutions. A key parameter, the Reynolds number (Re), elucidates this difference:

$$\text{Re} = \frac{du\rho}{\mu}$$

where d is the characteristic length scale of the channel and u , ρ , and μ are the velocity, density, and dynamic viscosity of the fluid, respectively. Microfluidic mixing is not intrinsically efficient due to the extremely low Re (typically <100) of laminar microfluidics in a simple flat channel with submillimeter size,⁴⁶ where mixing mainly relies on molecular diffusion at the interface and requires a rather long flow path to achieve intensive mixing.⁴⁷ Laminar microfluidics is advantageous to fabricating molecular patterns and layered structures.^{48,49} Besides, researchers have developed advection/turbulence-based micromixers to improve mixing by shortening the mixing length to centimeter scales and the mixing time down to submillisecond levels. Such mixers possess advantages of not only fast/intensive mixing along with rapid heat/mass transfer, but also easy management of the device, parameters, and environment, paving the way toward applications including but not limited to chemical synthesis.

Strategies toward enhanced micromixing are either passive or active. Active micromixers requiring external perturbation

energy are less frequently used in μ Syn. They are categorized with respect to the type of input energy (*e.g.*, pressure field and ultrasound), which is well discussed in existing reviews.⁵⁰ Passive mixing relies on rationally designed micromixers to restructure the flow to generate turbulence with maximized contact surface area. Passive micromixers generally appear as designed channel geometries. Strategies include Y/T-shaped channels, parallel/sequential lamination, hydrodynamic focusing, and chaotic advection.⁵¹ A serpentine laminating mixer (SLM) promotes micromixing in a synergistic mechanism of splitting/recombination and chaotic advection (Fig. 2A).⁵² The successive double-layered F-shaped mixing units and the 3D serpentine path contribute to the lamination and advection effects, respectively. The required mixing length λ is about 20 times shorter than that for the T-type micromixer at similar Re ($\lambda \approx 6 \text{ mm}/130 \text{ mm}$ for the SLM/T-type mixer with $\text{Re} \approx 2.28$).

Hydrodynamic focusing (HF) applies a central/sheath flow pair with preset volumetric flow rate ratios. We have developed a facile method to fabricate 3D origami microchips with enhanced HF.¹⁵ We can obtain both arc and double spiral geometries by simply folding a flat polydimethylsiloxane (PDMS) channel (Fig. 2B). The origami chips significantly reduce the mixing time thanks to their winding shapes. With a flow rate of 2.5 mL h^{-1} , the mixing time in the flat, arc, and double spiral channels is 29, 16, and 14.5 ms, respectively. The double spiral structure also allows efficient mixing when inserted as a part of a flat microchip *via* similar HF mechanisms.⁵³

Chaotic advection refers to multi-directional transport of substances in the moving fluid. Microchannels with inserted obstacles represent a model design to induce such phenomena. The staggered herringbone structure significantly enhances microfluidic mixing (Fig. 2C).⁵⁴ The confocal images show the vertical cross-sections of a channel with two fluorescent streams injected on either side of a clear solution. The raised herringbone structure serves as the embedded barrier to generate chaotic advection, which reduces the length required for 90% mixing by a factor of 100 compared to a smooth channel. A 3D manifold micromixer inserts layered crossing tubes into the microchannel to generate advection.⁵⁵

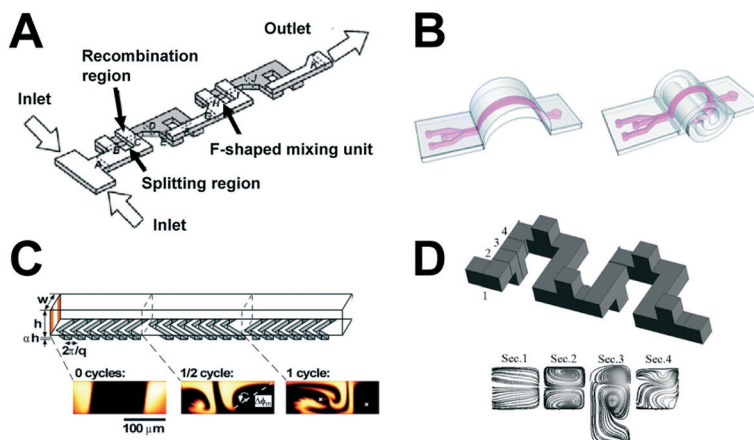


Fig. 2 Passive mixing strategies applied in designed microreactors. (A) A serpentine laminating mixer (SLM) combining splitting/recombination and chaotic advection mechanisms. Reprinted from ref. 52. Copyright 2005 Royal Society of Chemistry. (B) Arc and double spiral origami chips obtained by manual folding of a flat PDMS channel. Reprinted from ref. 15. Copyright 2013 Royal Society of Chemistry. (C) A staggered herringbone mixer with one-and-a-half cycles. The confocal images show the vertical cross-sections of a channel with two fluorescent streams injected on either side of a clear solution. Scale bar = 100 μm . Reprinted from ref. 54. Copyright 2002 The American Association for the Advancement of Science. (D) Design of the 3D stainless steel micromixer. The flow path includes a square-wave structure and periodic cubic grooves. The bottom shows the computational fluid dynamics simulation result of the streamlines at different sections labeled 1–4. Reprinted from ref. 57. Copyright 2011 Elsevier.

By realigning the fluid in many directions, a channel length of 250 μm is enough to complete 90% mixing under optimized conditions. Channels with 2D curved shapes (*e.g.*, the Tesla mixer⁵⁶) and 3D grooves also benefit advection generation. The wave-like channel path with periodic cubic grooves can stretch and compress the vortices toward intensive mixing (Fig. 2D).⁵⁷ The similar 3D serpentine design allows manipulation of ultrafast reaction kinetics.⁴⁰

Droplet-based systems (*e.g.*, suspended microdroplets or slugs) are widely adopted in μ Syn, with distinct mixing profiles compared to microchannels. Mixing in droplet microfluidics benefits from the geometrical confinement of the droplet itself, while the channel shape also plays a part, which causes the recirculating flow *via* contact with the droplet surface.^{58,59} The winding channel networks allow millisecond mixing within picolitre plugs, which is attributable to the unsteady recirculating flow generated upon droplet movement.⁵⁹ This work also demonstrates the spontaneous merging/splitting of pairs of plugs by inserting an incorporating branching point downstream the droplet generator, which is critically requisite to droplet microreactors.²⁶

3 Synthesis in microreactors: improved performance in various aspects

Microreactors or microchips are flexible in design, fabrication, operation, and integration. Various substrates like glass, silicon, polymers, and metals are available for making microreactors.⁶⁰ Photolithography,⁶¹ dry/wet etching,^{62,63} hot embossing,⁶⁴ laser ablation,⁶⁵ and so forth are all useful in fabricating designed microstructures on flat substrates.

Sealing methods include plasma treatment,⁶⁶ ultrasonic welding,⁶⁷ anodic bonding,⁶⁸ and thermal bonding.⁴⁰ Glass/silicon, metals (*e.g.*, aluminum and stainless steel), thermosets (*e.g.*, polyimide), and perfluorinated thermoplastics (*e.g.*, perfluoroalkoxy alkane) are applicable in organic synthesis due to the following advantages: (i) inertness against aqueous/organic solvents; (ii) ability to withstand high/low temperatures and high pressures; (iii) good transmission of light (both convenient for monitoring the reaction process and essential to photo-assisted synthesis).^{22,40,69–71} For synthesis of materials like nanoparticles and microfibers, glass and polymers (PDMS, in particular) are frequently used.^{23,35,49} Diverse designs of microreactors, including winding tubes,⁷¹ serpentine channels,⁷² origami chips,¹⁵ and 3D structures,⁷³ are feasible for chemical synthesis. In some cases, physicochemical modification is required such as loading a layer of catalytic beads or inserting a slice of membrane. Here, we highlight the improved performance of microreactors in various situations, emphasizing on their smart design and fabrication that can benefit specific uses.

3.1 Heading to target products: multistep and multiphase synthesis

A synthetic process usually includes many steps, which have to be carried out stepwise with conventional batch methods. However, a multistep process can be facilely completed in a fast and continuous manner with designed microreactors, thus simplifying the whole procedure with improved efficiency. To perform such processes in microfluidics, one needs to introduce the reagents in the right order and orchestrate the reactions of each step, as well demonstrated in a five-step synthesis of a [¹⁸F]-labeled probe in an integrated

microchip.⁷⁴ Meanwhile, components like inlets, mixers, separators, and outlets require rational design and arrangement, which is represented by a three-step synthesis of carbamates from acid chlorides (Fig. 3A).²⁰ The chain-like microsynthesizer contains three serpentine microreactors and two microseparators: $\mu R1-3$ to generate organic azide, isocyanate, and carbonate in sequence and $\mu S1$ and 2 for quantitative separation of organic/aqueous streams and N_2 /liquid streams. The reactor/separator network also implies an integration strategy as further illustrated in recent advances,²⁴ and the reaction parameters of each part can be set and regulated separately.⁷¹

The above principles and superiorities of microreactors for multistep synthesis also work well in preparing micro/nanomaterials with hybrid structures.^{14,21} Batch synthesis of core-shell micro/nanostructures includes several separate steps. For instance, a pathway to poly(lactic-co-glycolic acid) (PLGA) core/lipid shell nanocomposites, a frequently used drug delivery system in cancer therapeutics, is to prepare PLGA nanoparticles and lipid capsules separately and then combine them together. This method suffers from two major limitations: (i) the difficulty and poor controllability in fabricating the reverse micelle; (ii) complex operations and purifications throughout the assembly process.⁵ We have developed a three-stage double spiral microchip for multistep assembly of core-shell nanoparticles in a continuous manner (Fig. 3B).²¹ The first stage has two side inlets for introducing PLGA/lipid precursors and one central inlet for water injection, where the water cores appear upon the rapid assembly of lipid molecules. The generated cores directly flow to the second stage to form the PLGA shells. At the third stage, the water core/PLGA shell composites undergo intensive mixing with the injected lipids in the double spiral mixer to form the lipid layers. It is noteworthy that no purification step is required throughout the whole process due to the narrow size distribution of the nanoparticles obtained in each stage, thus, the whole procedure is greatly simplified.

Multiphase synthesis such as heterogeneous catalysis requires the reactants/catalysts to sufficiently converge at the phase interface and undergo effective interactions, which is achievable by using microreactors with intrinsic advantages such as large surface-to-volume ratios and enhanced heat/mass transfer. For solid-supported catalysis, a general strategy is to immobilize the catalysts on the inner wall of microreactors to interact with the gas/liquid flow, as typically illustrated in Fig. 4A.⁷⁵ The immobilized Pd catalysts promote the hydrogenation of benzalacetone in the liquid/gas stream (Fig. 4A, bottom). Desired products quantitatively appear within 2 minutes due to the fast and effective interactions among the three phases, which is ascribed to the extremely large interfacial area and short diffusion path in the narrow channel space. This strategy is also applicable to heterogeneous enzyme-catalyzed polymerization (Fig. 4B).²² The ring-opening polymerization of ϵ -caprolactone to polycaprolactone (PCL) (Fig. 4B, bottom) proceeds in an aluminum microreactor upon heating with enzyme-loaded beads densely packed on the bottom of the microchannel. The microdevice has higher catalyst surface area and improved transport properties compared to batch reactors, leading to faster reaction rates (apparent rate constants are 0.007 to 0.012 s^{-1} for microreactors and 0.0004 to 0.0008 s^{-1} for batch reactors) and higher PCL molecular weights (15 000 to 25 000 for microreactors and 5000 to 10 000 for batch reactors) at identical temperatures. The solid-supported systems eliminate the repetitive and labor-intensive separation of the reaction mixtures (e.g., recycling the catalyst), and can be easily compartmentalized for cascade reactions.⁷⁶

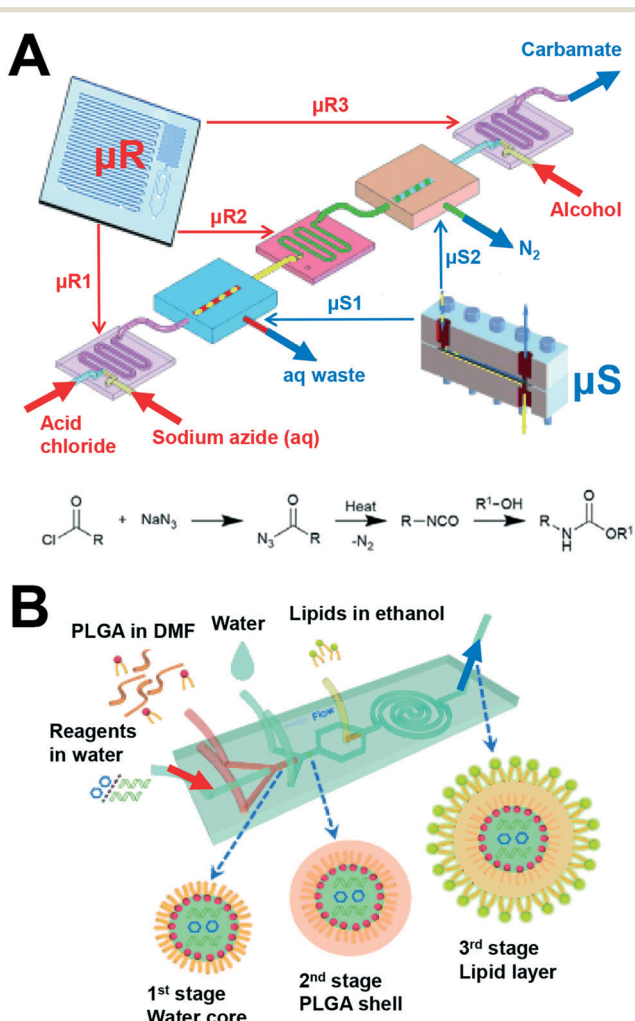


Fig. 3 Multistep synthesis in microreactors with/without purification after each step. (A) On-chip flow synthesis of carbamate involving multiple reactions and separations. $\mu R1-3$ are reactors generating organic azide, isocyanate, and carbonate, respectively. $\mu S1$ and 2 are separators for quantitative separation of organic/aqueous streams and N_2 /liquid streams. Reprinted from ref. 20. Copyright 2007 Wiley-VCH. (B) A three-stage double spiral chip for multistep synthesis of nanoparticles with controllable core-shell structures. The designed microchip eliminates the separation step due to the narrow size distribution of the nanoparticles obtained in each step, thus simplifying the whole synthetic process. Reprinted from ref. 21. Copyright 2015 Wiley-VCH.

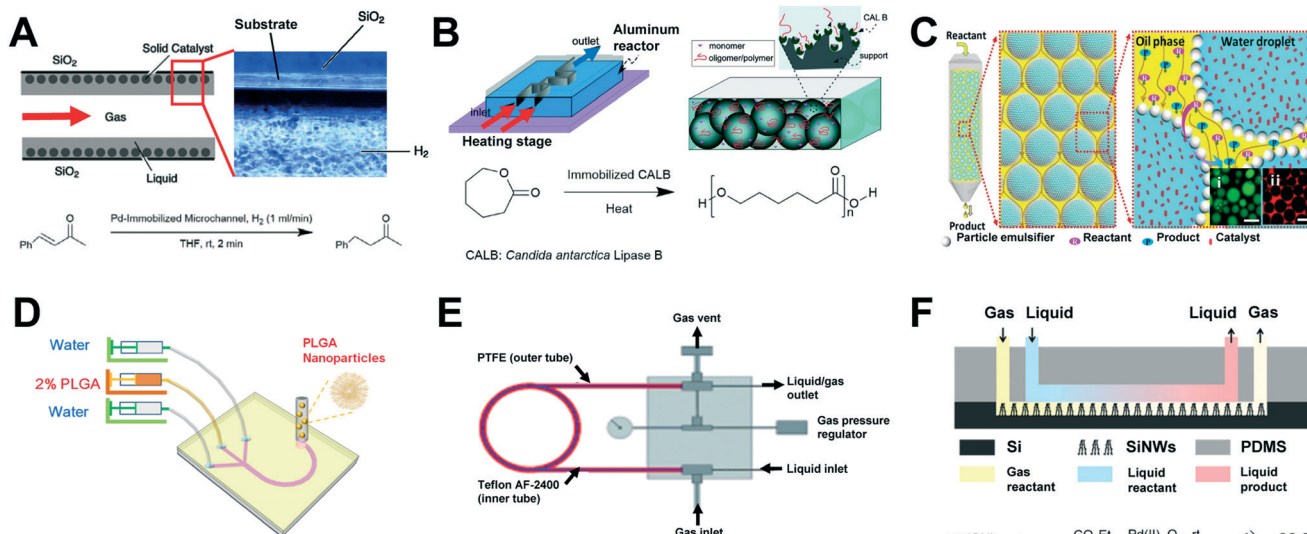


Fig. 4 Designed microreactors for multiphase transformations. (A) A device for conducting Pd-catalyzed hydrogenation of benzalacetone in a gas/liquid stream with the catalyst immobilized on the wall of the glass channel. Reprinted from ref. 75. Copyright 2004 The American Association for the Advancement of Science. (B) Schematic diagram of a microreactor applying packed beads for enzyme-catalyzed polymerization upon heating. Reprinted from ref. 22. Copyright 2011 American Chemical Society. (C) Schematic illustration of a column reactor with packed water-in-oil Pickering emulsion for organic-aqueous biphasic catalysis. Insets: Fluorescence confocal microscopy images of the water phase dyed with water-soluble FITC-dextran (i) and the oil phase dyed with oil-soluble Nile red (ii). Scale bar = 100 μm . Reprinted from ref. 17. Copyright 2016 American Chemical Society. (D) A microfluidic tubing method for biphasic synthesis of PLGA nanoparticles. The microchip can withstand high pressures and flow rates, which is essential to synthesizing small-size PLGA nanoparticles. Reprinted from ref. 66. Copyright 2014 Royal Society of Chemistry. (E) A tube-in-tube membrane microreactor for gas/liquid reactions. Reprinted from ref. 84. Copyright 2011 Wiley-VCH. (F) A silicon nanowire-based, membrane-free microreactor for the oxidative Heck reaction. Reprinted from ref. 85. Copyright 2016 American Chemical Society.

Batch methods generally apply mechanical agitation that consumes much space and energy to mix miscible/immiscible liquid phases, which is avoidable in microreactors due to the enhanced reaction interface. μ Syn with liquid/liquid systems is widely explored using fluids and droplets/slugs as reagent carriers,^{66,77,78} among which the organic-aqueous system is extensively adoptable due to its ability to carry both water-soluble and oil-soluble reagents. A column reactor with a packed water-in-oil Pickering emulsion allows organic-aqueous catalysis to proceed continuously with improved efficiency (Fig. 4C),¹⁷ where the silica nanospheres act as emulsifiers to generate compartmentalized water droplets (inset, i) in oil with hydrophilic catalysts dispersed in them. The “immobilized” catalysts then transform the reactants dissolved in the oil film (inset, ii) to the products. The water/oil interface serves as a novel conceptual microscale “reactor” driving the conventional organic-aqueous catalysis in a more sustainable way with up to 10-fold reaction efficiency enhancement. Multiphase synthesis of micro/nanomaterials in microfluidics is also feasible, especially for polymer-derived nanoparticles.^{77,79,80} We have performed microfluidic biphasic nanoprecipitation of PLGA in dimethylformamide upon the hydrodynamic focusing of water, which enables facile assembly of functional nanoparticles for biomedical applications.^{13,15,21,23,53,66,80,81} A notable case involves a microfluidic tubing method for PDMS chip fabrication as shown in Fig. 4D.⁶⁶ The microchip can withstand high pressures up to 4.5 MPa and flow rates up to 410 mL h⁻¹, which is essential

to synthesizing small PLGA nanoparticles (diameter <100 nm) with good dispersion. This work also highlights the importance of microchip fabrication in μ Syn.

Gas/liquid systems are also transplantable to microfluidics, avoiding the use of extreme measures (e.g., high pressure or supercritical conditions) to promote gas diffusion into the liquid phase. A simple design is to pump the liquid/gaseous phases simultaneously through a single channel microreactor to form segmented⁸² or annular flows (e.g., the three-phase system in Fig. 4A) with large interfacial contact area and short diffusion length. Membrane microreactors also gain much attention in performing gas/liquid reactions, which employ thin gas-permeable membranes to separate the two phases.⁸³ A typical example applies the tube-in-tube configuration by positioning the gas-permeable Teflon AF-2400 tubing (filled with the substrate stream) within the larger-diameter PTFE tube (filled with the gas flow) (Fig. 4E).⁸⁴ However, in view of the inherent drawbacks of membrane-based flow systems such as limited diffusion rates, the membrane-free microchemical system has recently emerged (Fig. 4F).⁸⁵ The superamphiphobic silicon nanowires (SiNWs) on the bottom wall prevent the penetration of the upper liquid stream into the lower gas stream, preserving the integrity of the two phases with improved mass transfer at the interface. An oxidative Heck reaction is performed as the model gas/liquid synthesis (Fig. 4F, bottom) with improved conversion against the traditional PDMS membrane microreactor.

3.2 Controlling what is going on: manipulating the flow, then the products

An ideal platform for synthesis is more than just a vessel for production, but also a tool for control. Batch reactors with large size and stepwise operation show mediocre performance in this aspect due to the difficulty in precisely modulating the reaction conditions and schemes. A number of parameters including temperature, pressure, the stoichiometric ratio, and catalyst can contribute to the quantity and quality of the product. For μ Syn, however, there is a unique control dimension, the flow, which mainly includes the flow rate, flow path, residence time, reagent transport, and so forth. Microfluidics enables facile manipulation of the synthesis within the flow by tuning these conditions, including (i) temperature control by introducing heating elements like the bath, (ii) flow rate control with programmable syringe pumps (also works in modulating the stoichiometric ratio and the residence time), (iii) flow path control by varying the geometry of microreactors, and (iv) reagent transport control by injection at precise time intervals or *via* inlets at desired locations. As a gift from microfluidic technology, flow manipulation has tremendous potential in making molecules and materials with tunable structures, properties, and functions.

Simply dipping microreactors in a water/oil bath enables precise control of the temperature that the flow actually “feels” thanks to their small size and rapid heat transfer. Meanwhile, temperatures at different parts/regions can be managed individually, which further improves the flexibility in handling complex processes.^{14,71,86} Temperature control in microreactors ensures relatively steady reaction environment and equilibrium that help to improve the yield of desired products. A notable case utilizing a cooling bath (-40°C) and a sonication bath (60°C) in separate steps allows regioselective arylation of fluoro- and trifluoromethyl-substituted arenes and pyridines.⁷¹ Varying the temperature in the range of 180 to 210°C also results in tunable size and emission characteristics of cadmium selenide (CdSe) nanocrystals.⁸⁷

The flow rate significantly affects the residence time, stoichiometric ratio, and mixing efficiency in microfluidics, which is critical to obtaining desired products with tunable structures and properties. We apply flow rate control to obtain polymer-lipid hybrid nanoparticles with tunable diameters.⁵³ As the flow rate varies from 41 mL h^{-1} to 246 mL h^{-1} , the size of the nanoparticles changes from 87 nm to 62 nm with a narrower size distribution. The flow rate can modulate the mixing ratio of different precursors to yield nanoparticles with varied size, surface chemistry, and drug loading.²⁷ Varying the flow ratio and total flow rate also allows fine tuning of the morphology and optical properties of noble metal nanoparticles.^{88–90}

Residence time, a widely used concept across many engineering disciplines, is easily tunable in microreactors by changing the flow rate and internal volume. It has a strong

impact on reaction kinetics and the yield distribution of different products toward desired chemo-,⁹¹ regio-,⁹² and stereoselectivity.^{93,94} The synchronous residence time between two parallel flow reactors allows parallel kinetic resolution of chiral saturated N-heterocycles with improved efficiency.⁹³ Meanwhile, residence time in microfluidics can reach the submillisecond level, which is beneficial for regulating short-lived species and processes known as “flash chemistry”.^{95,96} A 3D serpentine microreactor enables in-depth study and modulation of Fries rearrangement by control of residence time (Fig. 5).⁴⁰ It is fabricated *via* one-step thermal bonding of six polyimide layers (Fig. 5A). A model reaction displayed in Fig. 5B involves an aryllithium intermediate that can undergo rapid Fries rearrangement. The yield distribution of 2a and 3a is tunable by altering the residence time within a few hundreds of milliseconds (Fig. 5B). A residence time of 0.33 ms results in 91% yield of 2a from the original intermediate, indicating that the ultrafast mixing in the microreactor can outpace the rapid Fries rearrangement. The “flash” method also enables controlled selectivity in molecular synthesis that involves short-lived intermediates, which is nearly impossible for bulk methods due to their low mixing efficiency.⁹¹

Spatially manipulating the reagent transport scheme holds particular significance in preparing layered micro/nanostructures.^{21,23,49,81,97} A microchip with multiple core/sheath flow channels enables facile and controlled spinning of hollow microfibers with a varied number of cavities.⁴⁹ We synthesize PLGA core/lipid shell nanoparticles with tunable structures and properties by varying the reagent injection mode (Fig. 6).^{23,81} A two-stage PDMS microchip allows facile manipulation of flow transport and reagent delivery (Fig. 6A).²³ When PLGA is introduced at the first stage with the water sheath, it undergoes fast nanoprecipitation into the solid PLGA core, which serves as a rigid support for the lipids to self-assemble into a monolayer at the second stage. Since the lipid shell grows directly from the PLGA seed, no water exists between the PLGA core and the lipid layer (Fig. 6A, i, the P-L NPs). However, we obtain water-containing PLGA core/lipid shell nanoparticles by simply switching the injection site of PLGA and lipids (Fig. 6A, ii, the P-W-L NPs). The lipids form the micelle at the first stage. The PLGA nanoparticles generated at the second stage then diffuse into the cavity upon intensive mixing in the double spiral mixer. The hybrid structure has a water interlayer due to this diffusion process, which results in larger size and lower Young's modulus, implying higher flexibility (Fig. 6B). These nano-hybrids exhibit flexibility-regulated cellular uptake. The P-L NPs with lower flexibility are internalized more easily, which is ascribed to the mild shape deformation during cellular uptake as shown by the molecular dynamics simulations (Fig. 6B and C). We further demonstrate the fine tuning of the surface properties of PLGA-lipid hybrids using the same switching strategy. We obtain PLGA nanoparticles with monolayer/bilayer lipid shells with a single microchip (Fig. 6D). Similarly, the synthesized

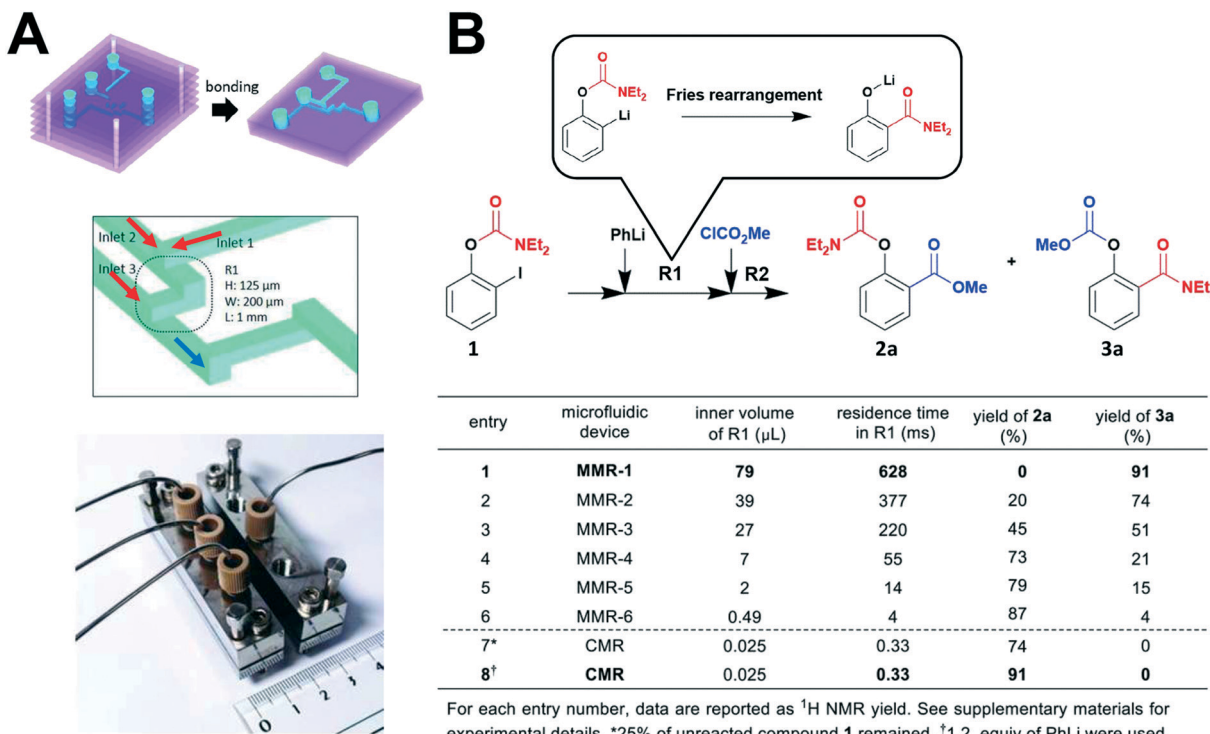


Fig. 5 Residence time control for product regulation. (A) Magnified scheme and optical image of a 3D serpentine microreactor fabricated with six layers of polyimide films *via* thermal bonding in one step. (B) Control of the product selectivity in Fries rearrangement through residence time variation. $\text{o-Iodophenyl diethylcarbamate}$ (**1**) is first mixed with PhLi through inlets 1 and 2 to generate the aryllithium intermediate that can undergo rapid Fries rearrangement. The intermediate then reacts with methyl chloroformate from inlet 3 to yield the final products (**2a** and **3a**). The inner volume decreases from the modular microreactor (MMR)-1 to the chip microreactor (CMR), resulting in decreased residence time and declined yield of the rearranged product. Reprinted from ref. 40. Copyright 2016 The American Association for the Advancement of Science.

nanoparticles show a clear variation in flexibility and behave differently when interacting with cells.⁸¹ It is worth noting that such an exquisite control of the flexibility while keeping all other parameters constant (*e.g.*, size, shape, and chemical composition) would be impossible for conventional methods.

3.3 Making it safer: hazardous reactions and green chemistry

Microreactors promote the development of synthetic chemistry toward sustainability and green synthesis with enhanced efficiency and improved safety.^{98–100} μSyn requires small quantities of reagents, and the residence time is often very short, which leads to minimal waste of resources. Meanwhile, microreactors with rather small size consume less space and energy compared to conventional reactors. Integrated microsystems, as further discussed in section 4, greatly improve the screening efficiency and significantly reduce manual operations. We highlight here the use of microreactors in handling hazardous conditions and chemicals, which again underscores the importance of microchip design and fabrication.

Safety has long been a major concern in synthetic chemistry due to the high risk of handling hazards. Microreactors with miniaturized size and strict control of reaction conditions enable safe management of elevated temperatures and

pressures. A silicon-based serpentine microchip can accelerate Pd-catalyzed Heck aminocarbonylation at high temperatures and pressures (Fig. 7A), which is rather difficult for batch reactors.⁶⁹ The microchip is fabricated *via* a solder-based technique and placed in an oil bath. It can stand temperatures up to 160 °C and pressures exceeding 100 bar, which enables rapid scanning of these parameters in a wide range. A droplet microreactor with a step increase in channel height enables continuous synthesis of CdSe nanocrystals at high temperatures around 300 °C.¹⁰¹

Intense heat release and accumulation can cause risks if mishandled in batch reactors. Microreactors with designed structures and enhanced mixing/heat transfer are suitable for exothermic reactions. Theoretical and experimental studies of the temperature profile of exothermic processes in microreactors provide design guidelines for heat management.^{102,103} A multilayered structured catalytic wall microreactor allows safe control of highly exothermic hydrogenation of acetylene to ethylene.¹⁰⁴ Besides, microreactors can act as effective tools to study the kinetics of fast exothermic reactions.¹⁰⁵ Modification of the substrate material like doping may improve the heat transfer performance of microreactors.¹⁰⁶

Continuous synthesis in microreactors avoids the storage of reaction intermediates that can be highly unstable or toxic, which enables safe treatment of hazardous chemicals.^{107,108}

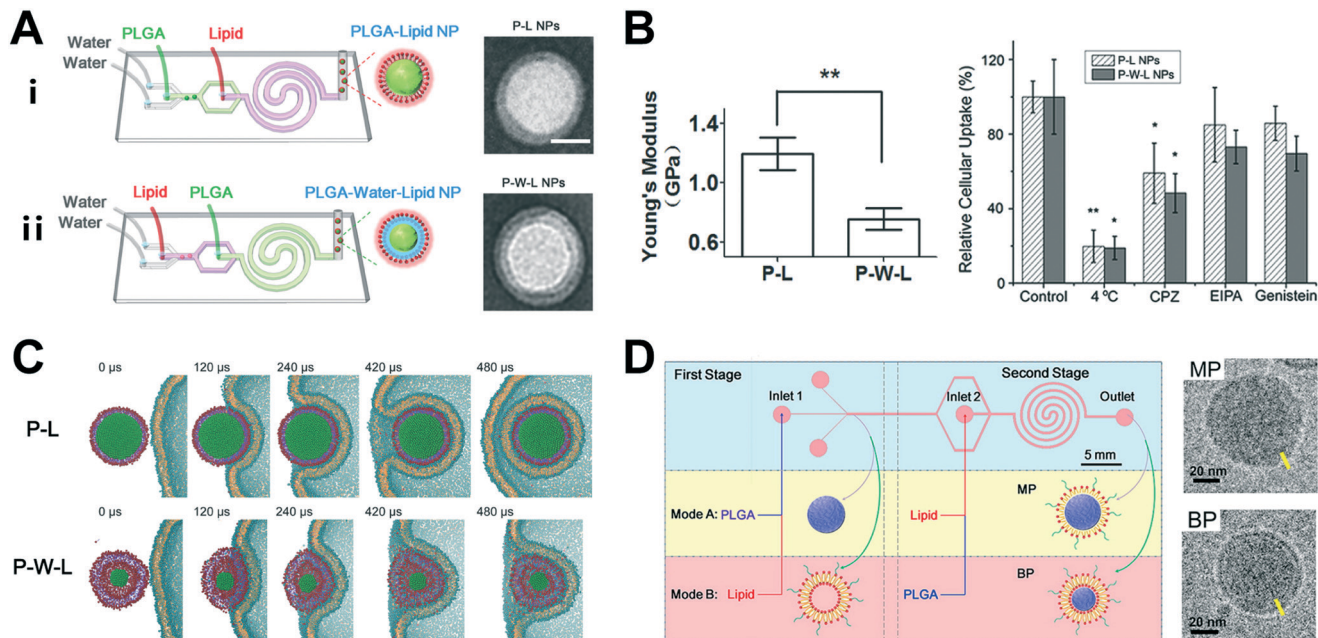


Fig. 6 Modulating the reagent transport scheme enables nanoparticle synthesis with tunable flexibility. (A) A two-stage microchip for making hybrid nanoparticles. Reagents can be introduced at different stages and inlets to obtain PLGA-lipid nanoparticles (P-L NPs, i) or PLGA-water-lipid nanoparticles (P-W-L NPs, ii). The TEM images show the interfacial water layer in P-W-L NPs. Scale bar = 25 nm. (B) Young's modulus and cellular uptake efficiency of the two kinds of nanoparticles. The P-L NPs with larger Young's modulus exhibit lower flexibility and higher uptake efficiency. (C) Flexibility-regulated cellular uptake of nanoparticles shown by molecular dynamics simulations. The P-L NPs undergo mild shape deformation and are internalized more easily. Reprinted from ref. 23. Copyright 2015 Wiley-VCH. (D) Modulation of the surface properties of PLGA nanoparticles using the same microchip design. By switching the injection site of PLGA and lipids, PLGA nanoparticles with monolayer/bilayer lipid shells (MP/BP) are obtained, which is confirmed by the TEM image. Scale bar = 20 nm. Reprinted from ref. 81. Copyright 2015 American Chemical Society.

A micro-total enveloped system (μ TES) can handle a carcinogenic compound, chloromethyl methyl ether (CMME) (Fig. 7B).²⁴ The key innovation lies in the use of SiNWs as membrane-free microseparators for highly efficient liquid/gas separation (Fig. 7B, middle) (for comparison, see Fig. 4F in which the SiNWs are embedded as the gas/liquid reactor). The μ TES generates CMME gas *in situ* at the first stage and separates it from the liquid reaction mixture with the SiNW separator. CMME moves directly to the next stage and reacts with other reagents to form the desired products. Finally, the unreacted CMME is eliminated by quenching. A case study applies the generated CMME to protect the acid-sensitive phenol group, and uses saturated NH₄Cl solution as the quencher (Fig. 7B, bottom). The *in situ* generation and consumption strategy enables safe treatment of hazardous chemicals in a closed and continuous manner with zero exposure to the environment. In another case, a highly toxic compound, hydrogen cyanide, is generated *in situ* and reacted downstream to synthesize the final product.¹⁰⁹

4 Beyond microreactors: integrated microsystems toward smart synthesis

Platforms such as the micro-total-analysis-systems (μ TAS) and lab-on-a-chip (LoC) have attracted worldwide attention with two distinct features: miniaturization and integration.

tion.^{46,110,111} In section 3, we highlight the improved performance and flexible applications of microreactors in diverse synthetic processes, which fully illustrates the superiority of their small size. However, regarding the development of μ Syn toward complex issues and practical translations, a single/simple microreactor unavoidably suffers from lack of throughput, offline analysis, and low automation levels. Besides, it requires complex manual intervention, from experimental operation to decision making, which leads to low efficiency and even mistakes. To settle these problems, the following integration strategies are urgently required: (i) internal integration, *i.e.*, improving the throughput of microreactors to integrate multiple processes into a single chip; (ii) external integration that refers to (a) integrating microreactors with other functional modules such as automatics, online/inline analytics, and feedback devices, and (b) combining multiple microreactors in parallel for large-scale synthesis. In a word, μ Syn is advancing toward an interdisciplinary field that attracts researchers from different backgrounds for a bright future.

4.1 From single to parallel: combinatorial synthesis and screening

Microfluidics with small size and high integration opens up new routes to combinatorial chemistry (CC). CC enables

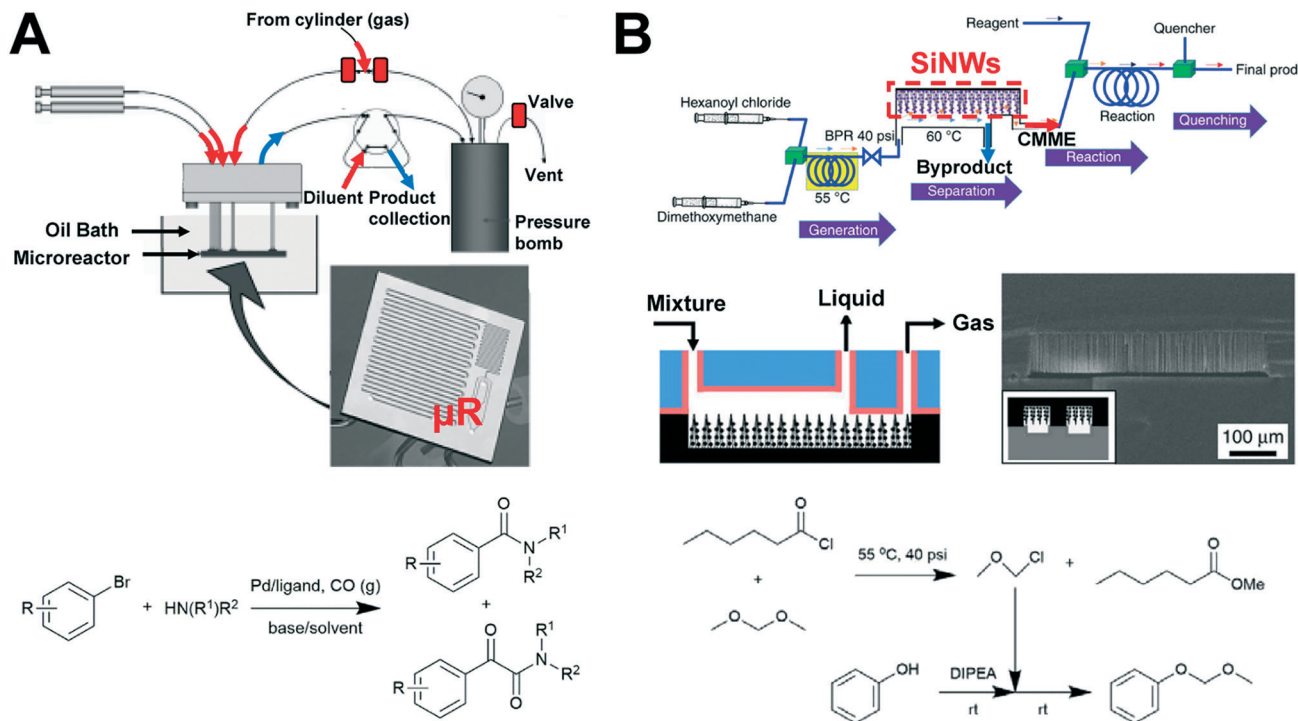


Fig. 7 Microreactors for handling hazardous conditions and chemicals. (A) Schematic diagram of a microreactor for accelerating Pd-catalyzed Heck aminocarbonylation at elevated temperatures and pressures. The silicon-based chip capable of standing pressures exceeding 100 bar is fabricated using a solder-based sealing technique and placed in a heated oil bath. Reprinted from ref. 69. Copyright 2007 Wiley-VCH. (B) Top: The micro-total enveloped system for safe treatment of carcinogenic reagents with silicon nanowires (SiNWs) as the microseparator. The red dashed lines mark the location of the SiNWs where the carcinogenic chloromethyl methyl ether (CMME, gas) is separated from the reactants and by-products (liquid). CMME is then reacted and eliminated in the next stages. Middle: The SiNW separator with one inlet and two outlets and the SEM image of its cross-sectional view. Scale bar = 100 μm . Bottom: The reaction scheme of the generation, consumption, and elimination of CMME. Reprinted from ref. 24. Copyright 2016 Nature Publishing Group.

rapid creation of libraries containing hundreds or thousands of products as a large database for subsequent discovery of either new drugs or novel materials.^{112,113} Conventional microreactors with low throughput cannot satisfy the requirements of CC. To realize improved throughput on a small space like a microchip, we need to (i) separate the candidate processes into independent injection units using either multiplex inlets or individual droplets, and (ii) build a screening system (either on-chip or off-chip) for rapid product analysis. This concept of integration has allowed the development of complex microreactors for CC, which well benefits their applications in sensing,¹¹⁴ drug discovery/delivery,^{6,25–28,115} and tissue engineering.³²

Reaction parameter scanning enables in-depth understanding of a model synthesis, which is important to the downstream production of functional molecules such as potential drugs. Integrated microfluidics allows rapid scanning of both continuous and discrete variables.^{25,26,34,116,117} Fig. 8A shows a multiplex high-throughput microchip for *in situ* click chemistry screening.²⁵ It comprises four parts: (i) a pair of microfluidic multiplexers with 2×16 individual inlets; (ii) a 150 nL rotary mixer; (iii) a 250 nL serpentine channel; (iv) a polytetrafluoroethylene (PTFE) tube reservoir. The operation of the circuit is computer-controlled using color-coded, pressure-driven valves labeled red, green,

and yellow. It can test 1024 individual reactions in parallel that involve 8 acetylenes, 16 azides, and 4 types of reaction conditions ($8 \times 16 \times 4 \times 2$ repetition = 1024). Separate slugs appear in the PTFE tube after all reactions are complete, followed by purification and offline screening with a mass spectrometer. The total reaction volume is approximately 400 nL, and the time required for a single click reaction is 17 s. The significance of this work lies in not only the large scale, but also its reduced time and reagent consumption, which fully embodies the dual advantages of microfluidic screening: throughput and efficiency. Droplet-based microfluidics also works in combinatorial synthesis.^{32,114,118,119} As shown in Fig. 8B, a library of picolitre microdroplets containing reagents A_{1-m} is prepared by flow focusing prior to injection into the PDMS device where the microdroplets containing reagents B_{1-n} are formed *in situ*.²⁶ The two kinds of droplets fuse together by electrocoalescence to generate the reaction mixtures, followed by off-chip analysis with liquid chromatography-mass spectrometry. A three-component Ugi-type reaction proceeds in this system by combinatorial mixing of 7 amines (reagent A) with 3 aldehydes (reagent B) while keeping the isocyanide constant (Fig. 8B, bottom). A 7×3 library is then obtained for screening possible thrombin inhibitors, which is scalable to make larger libraries.

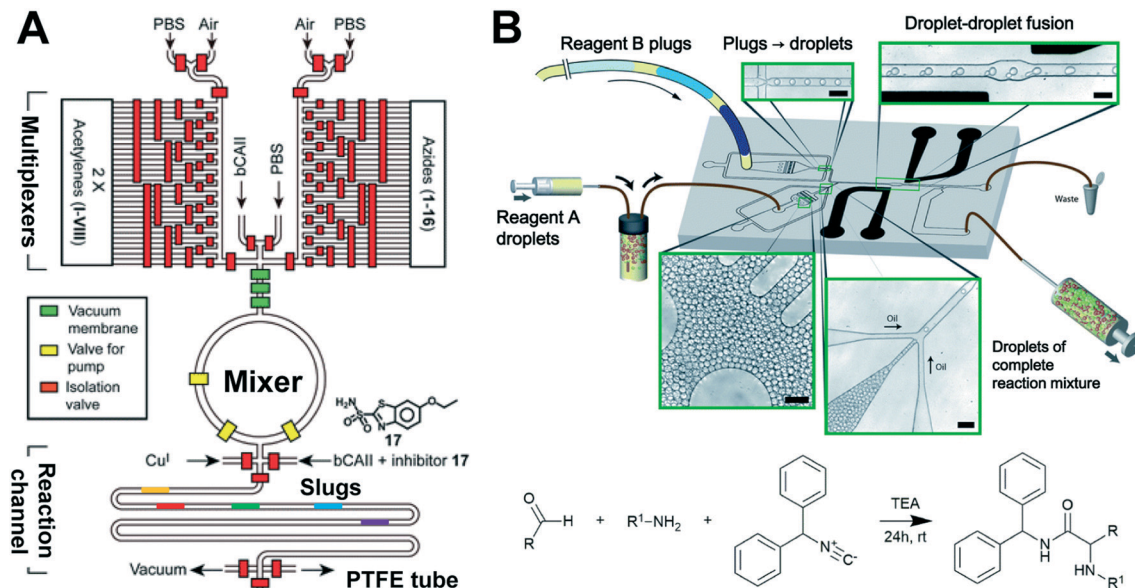


Fig. 8 Integrated microchips for combinatorial synthesis and large-scale screening. (A) Schematic diagram of an integrated microfluidic platform for large-scale *in situ* click chemistry screening. The device comprises four components: (i) a pair of microfluidic multiplexers regulating the inlets; (ii) a rotary mixer for reagent mixing; (iii) a serpentine channel to complete the mixing; (iv) a PTFE tube to serve as the reservoir. Separate slugs are generated in the PTFE tube after all reactions are complete and screened with an offline mass spectrometer. Reprinted from ref. 25. Copyright 2009 Royal Society of Chemistry. (B) Combinatorial synthesis in picolitre microdroplets. A library of droplets A_{1-m} is created and stored prior to use, and then injected to pair with droplets containing reagents B_{1-n} formed in the PDMS device. The reaction mixtures are screened with offline liquid chromatography-mass spectrometry. Scale bar = 50 μm . A three-component Ugi-type reaction is performed to screen possible thrombin inhibitors. Reprinted from ref. 26. Copyright 2012 Royal Society of Chemistry.

On-chip screening of functional micro/nanomaterials holds an attractive prospect in developing novel sensing platforms, drug delivery systems, and engineered tissues. Integrated microchips enable combinatorial synthesis of nanoparticles and rapid screening of multiple parameters such as size, surface chemistry, and function. A typical example includes a multi-inlet 3D micromixer followed by hydrodynamic focusing for synthesizing and screening PLGA-*b*-polyethylene glycol (PLGA-PEG) nanoparticles.²⁷ A number of PLGA-PEG precursors are injected *via* different inlets, mixed at various ratios *via* flow rate control, and then precipitated to form the library of nanoparticles (Fig. 9A). Four screening modes are available to realize varied size, surface charge, ligand density, and drug loading: (i) mixing PLGA-PEG precursors with different PLGA molecular weights; (ii) mixing the precursors with different functional groups on the PEG block; (iii) mixing the precursors with/without the targeting ligand; (iv) mixing the precursors with the drug and the solvent. The obtained nanoparticle libraries are screened with off-chip instruments and cell assays. The microfluidic platform allows rapid development and screening of nanoparticles as potential drug carriers. In another case, a combined microsystem including a digital droplet generator and a microfluidic cell culture array allows rapid screening of supramolecular nanoparticles (SNPs) (Fig. 9B).²⁸ Building blocks of the SNPs consist of four modules: proteins, genes, ligands, and scaffolds. Altering the ratios among these modules generates a combinatorial library of SNPs. The microchip can automatically prepare 375 formulations of SNPs in 1 h. The on-chip cell ar-

ray allows *in situ* screening of the synthesized SNPs, which significantly improves the efficiency of *in vitro* screening of drug delivery systems, and offers a promising strategy of combining microsynthesizers with cells/organs-on-chips for evaluating the bio-effect of molecules and nanomaterials.

4.2 From simple to smart: automation, real-time monitoring, and feedback

A smart platform is assumed to make the product and optimize the yield without human intervention. Automations play a major role in such devices that frees researchers from laborious work. Several automated systems are well established for microfluidic applications ranging from biomedical detection to chemical synthesis.^{29,120} Automation improves the stability and efficiency of μ Syn, which is significant to massive production and clinical/industrial translations.^{30,121} It is particularly useful in complex microreactors with multiple pumps/valves for regulating multistep processes or parallel syntheses.²⁵ Automated synthesis of small compounds,¹²² nucleic acids,¹²¹ peptides,¹²³ proteins,¹²⁴ and nanoparticles¹²⁵ is under extensive exploration in microreactors. Program control is essential to automated microsystems, which ensures all modules, including the injection system, micromixer/reactor, analytics, and feedback, to orchestrate in a well-organized manner.

Conventional batch/micro synthesis generally adopts external instruments to characterize the product, which is expensive and consumes large amounts of samples. Researchers

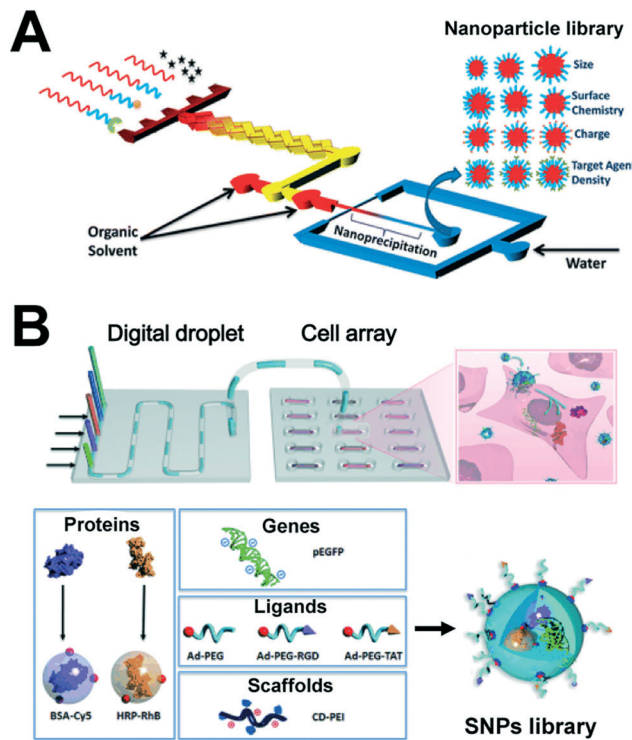


Fig. 9 On-chip screening of functional nanomaterials for biomedical applications. (A) Schematic illustration of a multi-inlet, 3D micromixer for synthesizing and screening PLGA-*b*-polyethylene glycol nanoparticles. Four screening modes are available for combinatorial synthesis of nanoparticles with varied size, surface charge, ligand density, and drug loading. Reprinted from ref. 27. Copyright 2013 American Chemical Society. (B) A combined microsystem for on-chip screening of supramolecular nanoparticles (SNPs). The integrated microchip contains a digital droplet generator and a cell array chip. The building blocks of the SNPs consist of four modules: proteins, genes, ligands, and scaffolds. The on-chip cell array allows *in situ* screening of the synthesized SNPs. Reprinted from ref. 28. Copyright 2016 Wiley-VCH.

have launched great effort to combine microsynthesizers with real-time analytics for process monitoring, which can be cate-

gorized as online or inline to probe reactions within or downstream the reaction zone. Optical sensors (*e.g.*, sensors based on absorption,¹²⁶ emission,⁴¹ scattering,^{127,128} and polarization¹²⁹ of light), chromatography,^{130,131} and mass spectrometry^{132,133} have been developed in such systems. However, problems exist in the interface of the reactor/detector network, especially for chromatography and mass spectrometry-based methods. The rather limited light path length in microdevices also makes it challenging toward high sensitivity with optical sensors. Gas bubbles that may appear in the flow have an adverse effect on nearly all analytics.

Generally, inline analytics probes reactions at equilibrium (*e.g.*, accomplished/quenched mixtures), with static information of product formation. Fig. 10A shows a microchip with high-pressure liquid chromatography (HPLC) for studying stereoselective transformations (*e.g.*, the intramolecular hetero-Diels–Alder reaction).¹³⁰ The reaction channel seamlessly interconnects with the HPLC column in a dead-volume free manner, which further links to the mass spectrometer *via* an electrospray ionization emitter. Incorporation of the downstream ultraviolet-visible spectrophotometer allows the monitoring of photocatalytic degradation.¹²⁶ The sample/reference cell has a length of 10 mm for light propagation. The flow-based device avoids complicated washing steps because the samples can refresh the cells themselves. Online/inline analytics is also applicable to segmented flow systems. A droplet reactor with inline surface-enhanced Raman spectroscopy (SERS) enables studying organic synthesis on the nanoliter scale.¹²⁷ It comprises a flow-focusing structure for droplet generation, a dispensing structure for mixing, and a downstream SERS detector, using silver nanoparticles as the enhancing agent.

Online detectors allow dynamic probing at desired positions within the reaction zone, and are suitable for quantifying fast reaction kinetics (*e.g.*, capturing short-lived intermediates). A typical work applies synchrotron-based infrared and X-ray beams for spectral mapping of gold nanocluster-catalyzed cascade dihydropyran synthesis, with a spatial

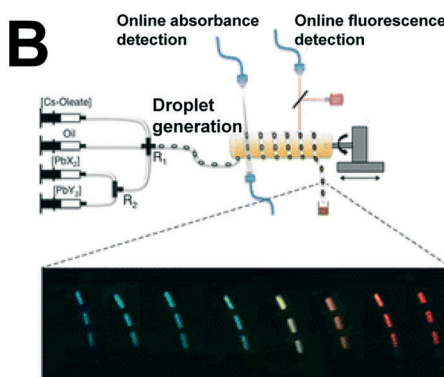


Fig. 10 Integration of microreactors with online/inline analytics. (A) Coupling of microflow synthesis and inline high-pressure liquid chromatography (HPLC) analysis on a single microfluidic device. The reactor outlet is interconnected with a packed HPLC column that is further linked to a mass spectrometer. Reprinted from ref. 130. Copyright 2016 Royal Society of Chemistry. (B) A droplet-based microfluidic platform for synthesis and real-time monitoring of cesium lead halide (CsPbX₃) perovskite nanocrystals. It includes an absorbance detector and a fluorescence detector, which enables *in situ* monitoring of the early stages of CsPbX₃ formation. Reprinted from ref. 41. Copyright 2016 American Chemical Society.

resolution of $15\text{ }\mu\text{m}$.¹³⁴ Online mapping of nanocrystal nucleation and growth is well demonstrated in microreactors.¹³⁵ A droplet-based microfluidic platform allows continuous synthesis and online monitoring of cesium lead halide (CsPbX_3) perovskite nanocrystals (Fig. 10B).⁴¹ It includes an absorbance detector and a fluorescence detector. The light travels in a tangential manner that matches the length of the reaction plugs (2 mm) to realize adequate sensitivity in absorbance. The integrated microsystem can monitor the early stages of CsPbX_3 formation (within the first 0.1–5 s) *in situ*, which allows fast and in-depth mapping of the parameters that govern the reaction kinetics and equilibrium. Unlike inorganic nanocrystals, probing self-assembled nanomaterials (e.g., lipid capsules) in real time can be difficult. A recent work applies the Förster resonance energy transfer strategy to visualize the self-assembly process in microfluidics.⁴²

Online/inline detectors can reduce the time and reagent consumption in combinatorial synthesis, and provide instant feedback on optimization. However, building a robot-like optimization system still remains challenging. The computer art with strong data processing facilitates the design of truly smart microsynthesizers with self-optimization capacity (*i.e.*, to “decide” which parameter to adjust based on the acquired

data), eliminating repetitive manual operations, especially when there is no prior information or model for reference (*e.g.*, the “from scratch” optimization).⁴⁵ Such devices generally contain four parts: (i) the computerized control system (preloaded with designed algorithms); (ii) the reagent transport system; (iii) the mixing/reaction region; (iv) the online/inline detection module (also see Fig. 1C).¹³⁶ Several intelligent algorithms (*e.g.*, the classical design of experimental methods¹³⁷) have been developed to interpret real-time data and adapt subsequent conditions.^{138,139} Pioneered by the smart synthesis of CdSe nanoparticles using an autonomous “black-box” microsystem (Fig. 11A),¹⁴⁰ the self-optimizing system based on microreactors is under broad exploration, with special interest in developing organic methodologies.^{33,34}

Constraint optimization is widely adopted in such devices to cope with complex variables, possibly without prior knowledge. It works in a parametric space with reasonably defined boundaries and outcomes. The CdSe synthesizer comprises a utility function, dissatisfaction coefficient (DC), with the emission wavelength and intensity as separate utility functions. Accordingly, three parameters, namely, temperature and flow rates of the Se and Cd precursors, are explored. The system applies the routine Stable Noisy Optimization by

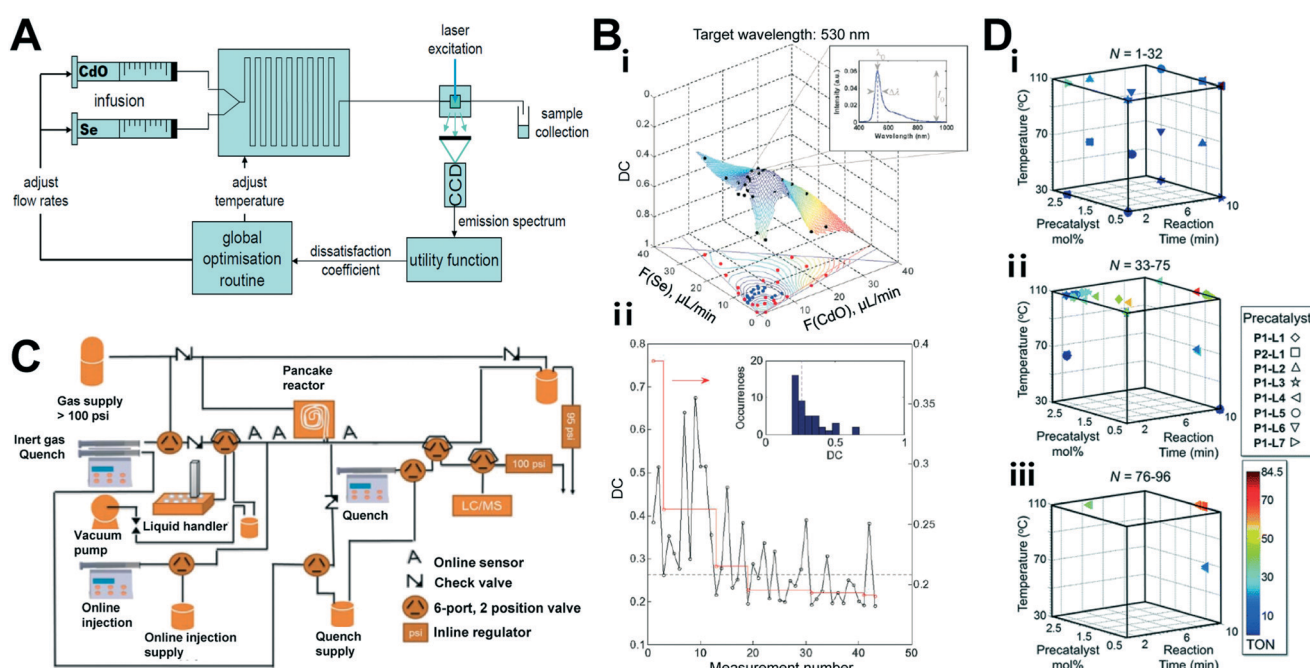


Fig. 11 Highly integrated and fully automated microplatforms for smart synthesis. (A) The design of the “black box” microsystem for robotic optimization of CdSe synthesis. (B, i) The result of flow rate screening at a fixed temperature of $220\text{ }^\circ\text{C}$. The red/blue markers show the specific reaction conditions sampled by the control algorithm, with the red and blue colors indicating corresponding dissatisfaction coefficient (DC) values that are, respectively, greater or smaller than the median value of 0.26. The black markers denote the DC value at each point. (B, ii) The variation in DC value (black markers) and λ_{best} (red markers) with the measurement number. Reprinted from ref. 140. Copyright 2007 Royal Society of Chemistry. (C) Schematic illustration of the droplet-based microsystem for automated Suzuki-Miyaura cross-coupling screening and optimization. Droplets are used here to screen both continuous and discrete variables. (D) Optimization routes followed by the automated system for a specific case, where (i), (ii), and (iii) refer to initialization, quadratic response surface refinement, and convergence, respectively. In a typical process, the system initiates by searching the extremes of the continuous variable experimental space (i) and then moves to interior points and progressively eliminates bad candidate catalysts based on the yield and turnover number (TON) (ii). This leads to iterative refinement until only P1-L4 remains. Finally, it tunes the catalyst loading until an optimal TON and an acceptable yield are achieved (iii). Reprinted from ref. 34. Copyright 2016 Royal Society of Chemistry.

Branch and Fit (SNOBF) as the effective algorithm to minimize DC. The two-dimensional result (*i.e.*, keep the temperature constant) finds a single optimum in the low flow rate region of the response surface, with the smallest DC value of 0.190 obtained at injection rates of 4.960 (for CdO) and 9.830 (for Se), respectively (Fig. 11B, i). The fluctuation of DC with the measurement number confirms the continual alternation between local and global searching of the SNOBF algorithm (Fig. 11B, ii). The more complicated 3D experiment further demonstrates the effectiveness of the system in simplifying and automating nanoparticle production.

With regard to organic synthesis, a recently developed, continuous flow-based system applies a modified Nelder-Mead simplex algorithm to optimize the palladium-catalyzed Heck–Matsuda reaction.³³ The temperature, residence time, reagent stoichiometry, and catalyst loading are optimized toward maximized yield, maximized productivity, and minimized cost. However, continuous flow systems are incompetent to optimize discrete variables (*i.e.*, variables that change discontinuously, *e.g.*, the precursors or catalyst ligands). Recently, a droplet-based feedback network allows simultaneous optimization of both continuous variables (*e.g.*, catalyst loading and reaction time) and discrete variables (*e.g.*, catalyst scaffold and ligand) in Suzuki–Miyaura cross-coupling reactions (Fig. 11C).³⁴ The optimization algorithm fed with the HPLC data mainly includes three stages (Fig. 11D): (i) searching the extremes/boundaries of the variable space; (ii) moving to the interior space and progressively eliminating inefficient candidates; (iii) tuning the catalyst loading until an optimal candidate appears. Such highly integrated and fully automated microsystems significantly accelerate the optimization process, drawing an inspiring prospect of applying

such platforms for smart manufacture in both the lab and industry.

4.3 From lab to industry: integration and scale-up strategies

For synthetic chemistry, the gap between academia and clinic/industry mainly lies in (i) quality control and (ii) production scale. Compared to batch reactors, microreactors have better batch-to-batch reproducibility and controllability. However, large-scale synthesis has long been a challenge for microfluidics, which has limited its applications in clinical trials and industry. Strategies to solve this problem include (i) improving the productivity of single microreactors^{35,36,73,141} and (ii) integrating multiple microreactors in parallel,^{38,39} which are critical to promote the translation of μ Syn.

The productivity of PDMS microchips for nanoparticle synthesis is quite limited due to their incompatibility with organic solvents and small molecules.^{142,143} Moreover, polymers like PLGA can aggregate on the hydrophobic walls and cause channel clogging.³⁵ Glass-based microreactors show improved performance in preparing hydrophobic materials in large quantities. A co-flow capillary device allows high-throughput synthesis of homogeneous polymeric nanoparticles due to its hydrophilic properties and coaxial flow feature (Fig. 12A).³⁵ It contains an inner tapered glass capillary inserted into an outer cylindrical one in a coaxially aligned manner. The inner fluid carrying aqueous solutions and the outer fluid carrying nanoparticle precursors flow in the same direction. The controlled microvortices and unsteady jetting enable fast mixing and uniform precipitation of the precursors, which also prevent polymer aggregation

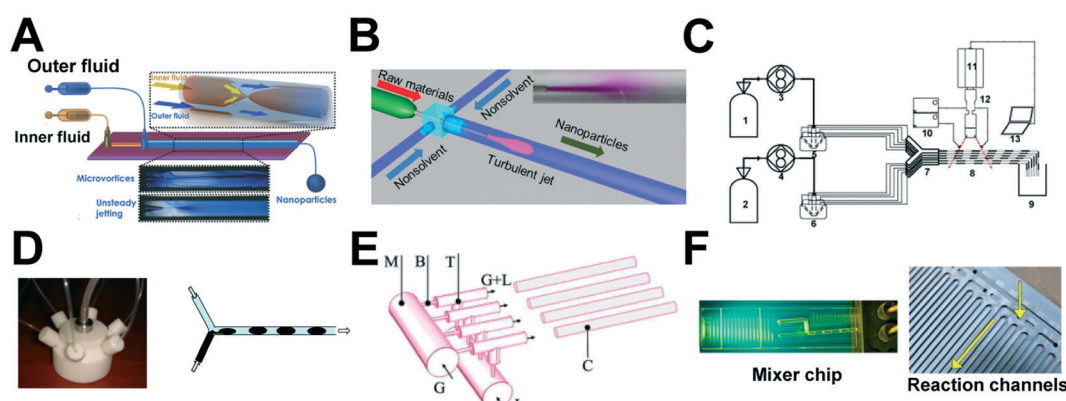


Fig. 12 Scale-up of microreactors for enhanced productivity. (A) Schematic illustration of a co-flow capillary device containing an inner fluid and an outer fluid. The controlled microvortices and unsteady jetting between the two fluids enable fast mixing and uniform self-assembly of nanoparticles. Reprinted from ref. 35. Copyright 2015 Wiley-VCH. (B) Schematic diagram and photograph of a coaxial turbulent jet mixer made of a syringe needle and a “T” tube fitting. Reprinted from ref. 36. Copyright 2014 American Chemical Society. (C) An integrated network of parallel microreactors for liquid-liquid reactions. The numbers refer to: (1 and 2) reservoirs, (3 and 4) pumps, (5 and 6) distributors, (7) Y mixers, (8) reaction channels, (9) collecting beaker, (10) light source, (11) camera, (12) optical microscope, and (13) laptop. (D) The distributor and Y-shape mixer. The distributors made of Teflon ensure uniform flow distribution into the parallel Y-shaped mixers for reactions. Reprinted from ref. 38. Copyright 2010 Elsevier. (E) Schematic diagram of a numbered-up gas-liquid micro/millireactor. Symbols used are: (G and L) gas and liquid inlets, (M) manifold, (B and T) barrier channels and T mixers, and (C) reaction channels. The gas and liquid reactants are split in the manifold and delivered to the parallel mixer chips and reaction channels. (F) Optical images of the mixer chip and reaction channels. Reprinted from ref. 39. Copyright 2012 Elsevier.

and result in high mass production rates up to 242.8 g d^{-1} . A similar coaxial turbulent jet mixer is easily available by inserting a syringe needle into a "T" tube mixer (Fig. 12B).³⁶ It exhibits a high production rate of drug-loaded polymeric nanoparticles up to 3 kg d^{-1} with good batch-to-batch reproducibility, which is directly applicable in *in vitro* experiments.

Increasing the number of elementary microreactors into a network is a direct and practical strategy for large-scale synthesis. The major challenge is flow distribution, which is dominated by many design parameters.¹⁴⁴ A model design for liquid–liquid reactions is shown in Fig. 12C.³⁸ It includes two single-phase flow distributors, six two-phase Y-shaped mixers, six capillary microreactors and a high-speed imaging system (Fig. 12C). The distributors made of Teflon ensure uniform flow distribution into the parallel Y-shaped mixers (Fig. 12D). A series of gas–liquid micro/millireactors are coupled in Fig. 12E.³⁹ The system mainly contains three parts: (i) the manifold for splitting and delivering the reagent fluids; (ii) the parallel barrier-mixer chips for mixing (Fig. 12F); (iii) the parallel reaction channels (Fig. 12F). It achieves a liquid flow rate up to 150 mL min^{-1} with less than 10% non-uniformity of flow delivery.

Actually, many other factors such as cost and applicability should also be considered in detail before pushing microsystems to the chemical industry. An obvious fact is that microreactors cannot afford all kinds of chemistries involved in current industries. Besides, manufacture of intact microchips on an industrial scale is rather challenging with existing technologies, which forms another barrier that hinders the clinical/industrial translation of μ Syn. In a word, there is still a long way to go to bring μ Syn out of the lab.

5 Discussion and perspective

Born as a microfabrication technique, microfluidics has attracted long-standing attention from the chemical society, with particular emphasis on altering the landscape of synthetic chemistry and relevant fields. Microfluidics offers a new concept/platform to conventional routes toward desired products, making the LoC accessible to handling complicated, dynamically changing systems. μ Syn empowers the LoC community to miniaturize huge networks of flasks or pipelines to make new chemicals, with the capacity of multiplexed screening and potential to achieve robotic systems. Like the μ TAS widely adopted in bioanalysis, μ Syn proves to be an exemplificative success broadening the concept of LoC to appeal and benefit synthetic chemists. Thus, the juncture where μ Syn and LoC meet and benefit each other can be summarized as: (i) μ Syn leads a new type of LoC focusing on chemical changes; (ii) beyond the simple " $A + B = C$ " format, LoC offers abundant functions to realize/improve current chemistries, and perhaps connects to a new world.

The development of μ Syn from simple microreactors to smart and integrated microsystems sheds light on the appealing future we are approaching. However, despite the tremen-

dous success we have achieved so far, great challenges are still in the way. In this section, we discuss the existing challenges and future opportunities of μ Syn from several aspects. We draw an ending for this review by providing the readers with critical and in-depth evaluation of the current state and future possibilities of this burgeoning field.

Technical concerns exist throughout all procedures involved in microfluidics-assisted synthesis. Selecting the right design, substrate, and sealing method for microchip fabrication has enormous impact on downstream applications, which deserves serious considerations when ready to engage in μ Syn. The intrinsic limitations of existing substrate materials (*e.g.*, PDMS) call for novel modifications/alternatives and packaging technologies for handling harsh conditions such as corrosive solvents/solutes, elevated temperatures/pressures, and high flow rates. Precise control of microfluidics also requires further improvement including microvalves/pumps, actuation strategies, and microdroplet generation/manipulation.

Microfluidics enables delicate investigation of the basics of physicochemical processes down to molecular levels. The primary topic is microfluidic mechanics, which includes (i) mechanical characteristics of microfluidics, (ii) factors/laws governing mixing and heat/mass transfer in microfluidics, and (iii) behaviors of molecules/particles in microfluidics. Ultrafast mixing in microfluidics makes it possible to track and modulate the process with higher resolution, uncovering the mechanisms that determine product formation. A major challenge is to shorten the residence/mixing time toward the lifetime of a synthesis as close as possible. Meanwhile, detection tools with high resolution/sensitivity are also required, especially for online mapping.

μ Syn is combining many subjects together to become an interdisciplinary science. Much room remains to broaden the applications of μ Syn: (i) trying more chemistries in microfluidics/microreactors; (ii) exploiting synthetic methodologies for controlled synthesis; (iii) preparing functional molecules/materials for sensing, imaging, cancer therapeutics, tissue engineering, and so forth; (iv) fabricating integrated devices for automated screening/optimization of model/unknown synthesis toward novel drugs/materials; (v) large-scale synthesis for clinical/industrial applications.

Every coin has two sides. Despite the great success brought by μ Syn in recent years, it is impossible to completely replace conventional batch methods at the current stage mainly because of (i) its limited productivity and applicability in many existing chemistries and (ii) technical obstacles in large-scale manufacture of microreactors. Researchers should focus on attaining optimal results with microfluidics, rather than eliminating batch reactors.

6 Conclusion

In conclusion, we have reviewed the development of microfluidics-based chemical synthesis to show its unique advantages in handling various situations and outlined the

inherent trend toward integrated systems as smart micro-synthesizers. We have no intention to involve all existing cases related to this field, but to present typical examples that reflect the merits and trends of μ Syn in certain aspects. We aim to provide strategic guidance for the rational design, fabrication, and integration of microsystems for synthetic use. Existing challenges and future opportunities are also critically evaluated. Microfluidics is guiding profound changes in many research fields including but not limited to chemical synthesis, leading to a bright future with infinite possibilities toward both laboratorial and industrial applications.

Conflicts of interest

There are no conflicts of interest to declare.

Acknowledgements

We thank the Ministry of Science and Technology of China (2013YQ190467), the Chinese Academy of Sciences (XDA09030305) and the National Science Foundation of China (81361140345, 51373043, and 21535001) for financial support.

References

- N. A. Afagh and A. K. Yudin, *Angew. Chem., Int. Ed.*, 2010, **49**, 262–310.
- S. Sengupta, D. Eavarone, I. Capila, G. L. Zhao, N. Watson, T. Kiziltepe and R. Sasisekharan, *Nature*, 2005, **436**, 568–572.
- A. Lew, P. O. Krutzik, M. E. Hart and A. R. Chamberlin, *J. Comb. Chem.*, 2002, **4**, 95–105.
- F. E. Valera, M. Quaranta, A. Moran, J. Blacker, A. Armstrong, J. T. Cabral and D. G. Blackmond, *Angew. Chem., Int. Ed.*, 2010, **49**, 2478–2485.
- M. P. Chelopo, L. Kalombo, J. Wesley-Smith, A. Grobler and R. Hayashi, *J. Mater. Sci.*, 2017, **52**, 3133–3145.
- Z. Chen, W. Li, G. Choi, X. Yang, J. Miao, L. Cui and W. Guan, *Sensors*, 2016, **16**, 1616.
- G. M. Whitesides, *Nature*, 2006, **442**, 368–373.
- J. Sun, Y. Xianyu and X. Jiang, *Chem. Soc. Rev.*, 2014, **43**, 6239–6253.
- X. Mu, W. Zheng, J. Sun, W. Zhang and X. Jiang, *Small*, 2013, **9**, 9–21.
- W. Pan, W. Chen and X. Jiang, *Anal. Chem.*, 2010, **82**, 3974–3976.
- Y. Lei, L. Tang, Y. Xie, Y. Xianyu, L. Zhang, P. Wang, Y. Hamada, K. Jiang, W. Zheng and X. Jiang, *Nat. Commun.*, 2017, **8**, 15130.
- P. Watts and S. J. Haswell, *Chem. Soc. Rev.*, 2005, **34**, 235–246.
- Q. Feng, J. Sun and X. Jiang, *Nanoscale*, 2016, **8**, 12430–12443.
- A. Abou-Hassan, O. Sandre, S. Neveu and V. Cabuil, *Angew. Chem., Int. Ed.*, 2009, **48**, 2342–2345.
- J. Sun, Y. Xianyu, M. Li, W. Liu, L. Zhang, D. Liu, C. Liu, G. Hu and X. Jiang, *Nanoscale*, 2013, **5**, 5262–5265.
- Y. Zhao, H. C. Shum, H. Chen, L. L. A. Adams, Z. Gu and D. A. Weitz, *J. Am. Chem. Soc.*, 2011, **133**, 8790–8793.
- M. Zhang, L. Wei, H. Chen, Z. Du, B. P. Binks and H. Yang, *J. Am. Chem. Soc.*, 2016, **138**, 10173–10183.
- A. R. Longstreet and D. T. McQuade, *Acc. Chem. Res.*, 2013, **46**, 327–338.
- C. Xu, X. Yang, X. Fu, R. Tian, O. Jacobson, Z. Wang, N. Lu, Y. Liu, W. Fan, F. Zhang, G. Niu, S. Hu, I. U. Ali and X. Chen, *Adv. Mater.*, 2017, **29**, 1603673.
- H. R. Sahoo, J. G. Kralj and K. F. Jensen, *Angew. Chem., Int. Ed.*, 2007, **46**, 5704–5708.
- L. Zhang, Q. Feng, J. Wang, J. Sun, X. Shi and X. Jiang, *Angew. Chem., Int. Ed.*, 2015, **54**, 3952–3956.
- S. Kundu, A. S. Bhangale, W. E. Wallace, K. M. Flynn, C. M. Guttman, R. A. Gross and K. L. Beers, *J. Am. Chem. Soc.*, 2011, **133**, 6006–6011.
- J. Sun, L. Zhang, J. Wang, Q. Feng, D. Liu, Q. Yin, D. Xu, Y. Wei, B. Ding, X. Shi and X. Jiang, *Adv. Mater.*, 2015, **27**, 1402–1407.
- A. K. Singh, D.-H. Ko, N. K. Vishwakarma, S. Jang, K.-I. Min and D.-P. Kim, *Nat. Commun.*, 2016, **7**, 10741.
- Y. Wang, W. Y. Lin, K. Liu, R. J. Lin, M. Selke, H. C. Kolb, N. Zhang, X. Z. Zhao, M. E. Phelps, C. K. Shen, K. F. Faull and H. R. Tseng, *Lab Chip*, 2009, **9**, 2281–2285.
- A. B. Theberge, E. Mayot, A. El Harrak, F. Kleinschmidt, W. T. Huck and A. D. Griffiths, *Lab Chip*, 2012, **12**, 1320–1326.
- P. M. Valencia, E. M. Pridgen, M. Rhee, R. Langer, O. C. Farokhzad and R. Karnik, *ACS Nano*, 2013, **7**, 10671–10680.
- Y. Liu, J. Du, J.-s. Choi, K.-J. Chen, S. Hou, M. Yan, W.-Y. Lin, K. S. Chen, T. Ro, G. S. Lipshutz, L. Wu, L. Shi, Y. Lu, H.-R. Tseng and H. Wang, *Angew. Chem., Int. Ed.*, 2016, **55**, 169–173.
- M. Peplow, *Nature*, 2014, **512**, 20–22.
- R. M. Maceiczyk, I. G. Lignos and A. J. deMello, *Curr. Opin. Chem. Eng.*, 2015, **8**, 29–35.
- B. J. Reizman and K. F. Jensen, *Acc. Chem. Res.*, 2016, **49**, 1786–1796.
- L. A. Bawazer, C. S. McNally, C. J. Empson, W. J. Marchant, T. P. Comyn, X. Niu, S. Cho, M. J. McPherson, B. P. Binks, A. deMello and F. C. Meldrum, *Sci. Adv.*, 2016, **2**, e1600567.
- D. Cortes-Borda, K. V. Kotonova, C. Jamet, M. E. Trusova, F. Zamattio, C. Truchet, M. Rodriguez-Zubiri and F.-X. Felpin, *Org. Process Res. Dev.*, 2016, **20**, 1979–1987.
- B. J. Reizman, Y. M. Wang, S. L. Buchwald and K. F. Jensen, *React. Chem. Eng.*, 2016, **1**, 658–666.
- D. Liu, S. Cito, Y. Zhang, C. F. Wang, T. M. Sikanen and H. A. Santos, *Adv. Mater.*, 2015, **27**, 2298–2304.
- J.-M. Lim, A. Swami, L. M. Gilson, S. Chopra, S. Choi, J. Wu, R. Langer, R. Karnik and O. C. Farokhzad, *ACS Nano*, 2014, **8**, 6056–6065.
- R. R. Hood and D. L. DeVoe, *Small*, 2015, **11**, 5790–5799.
- M. N. Kashid, A. Gupta, A. Renken and L. Kiwi-Minsker, *Chem. Eng. J.*, 2010, **158**, 233–240.

- 39 M. Al-Rawashdeh, F. Yu, T. A. Nijhuis, E. V. Rebrov, V. Hessel and J. C. Schouten, *Chem. Eng. J.*, 2012, **207–208**, 645–655.
- 40 H. Kim, K.-I. Min, K. Inoue, D. J. Im, D.-P. Kim and J.-i. Yoshida, *Science*, 2016, **352**, 691–694.
- 41 I. Lignos, S. Stavrakis, G. Nedelcu, L. Protesescu, A. J. deMello and M. V. Kovalenko, *Nano Lett.*, 2016, **16**, 1869–1877.
- 42 B. L. Sanchez-Gaytan, F. Fay, S. Hak, A. Alaarg, Z. A. Fayad, C. Perez-Medina, W. J. M. Mulder and Y. Zhao, *Angew. Chem., Int. Ed.*, 2017, **56**, 2923–2926.
- 43 A. K. Au, W. Huynh, L. F. Horowitz and A. Folch, *Angew. Chem., Int. Ed.*, 2016, **55**, 3862–3881.
- 44 P. Tseng, W. M. Weaver, M. Masaeli, K. Owsley and D. Di Carlo, *Lab Chip*, 2014, **14**, 828–832.
- 45 M. Rasheed and T. Wirth, *Angew. Chem., Int. Ed.*, 2011, **50**, 357–358.
- 46 H. A. Stone, A. D. Stroock and A. Ajdari, *Annu. Rev. Fluid Mech.*, 2004, **36**, 381–411.
- 47 P. J. A. Kenis, R. F. Ismagilov and G. M. Whitesides, *Science*, 1999, **285**, 83–85.
- 48 A. J. Gross, V. Nock, M. I. J. Polson, M. M. Alkaisi and A. J. Downard, *Angew. Chem., Int. Ed.*, 2013, **52**, 10261–10264.
- 49 Y. Yu, W. Wei, Y. Wang, C. Xu, Y. Guo and J. Qin, *Adv. Mater.*, 2016, **28**, 6649–6655.
- 50 C.-Y. Lee, C.-L. Chang, Y.-N. Wang and L.-M. Fu, *Int. J. Mol. Sci.*, 2011, **12**, 3263–3287.
- 51 L. Capretto, W. Cheng, M. Hill and X. Zhang, *Top. Curr. Chem.*, 2011, **304**, 27–68.
- 52 D. S. Kim, S. H. Lee, T. H. Kwon and C. H. Ahn, *Lab Chip*, 2005, **5**, 739–747.
- 53 Q. Feng, L. Zhang, C. Liu, X. Li, G. Hu, J. Sun and X. Jiang, *Biomicrofluidics*, 2015, **9**, 052604.
- 54 A. D. Stroock, S. K. W. Dertinger, A. Ajdari, I. Mezic, H. A. Stone and G. M. Whitesides, *Science*, 2002, **295**, 647–651.
- 55 T. W. Lim, Y. Son, Y. J. Jeong, D.-Y. Yang, H.-J. Kong, K.-S. Lee and D.-P. Kim, *Lab Chip*, 2011, **11**, 100–103.
- 56 C. C. Hong, J. W. Choi and C. H. Ahn, *Lab Chip*, 2004, **4**, 109–113.
- 57 Y. Lin, X. Yu, Z. Wang, S.-T. Tu and Z. Wang, *Chem. Eng. J.*, 2011, **171**, 291–300.
- 58 H. Song, J. D. Tice and R. F. Ismagilov, *Angew. Chem., Int. Ed.*, 2003, **42**, 768–772.
- 59 H. Song, M. R. Bringer, J. D. Tice, C. J. Gerdts and R. F. Ismagilov, *Appl. Phys. Lett.*, 2003, **83**, 4664–4666.
- 60 K. Ren, J. Zhou and H. Wu, *Acc. Chem. Res.*, 2013, **46**, 2396–2406.
- 61 G. M. Whitesides, E. Ostuni, S. Takayama, X. Y. Jiang and D. E. Ingber, *Annu. Rev. Biomed. Eng.*, 2001, **3**, 335–373.
- 62 J. Garra, T. Long, J. Currie, T. Schneider, R. White and M. Paranjape, *J. Vac. Sci. Technol., A*, 2002, **20**, 975–982.
- 63 A. Grosse, M. Grewe and H. Fouckhardt, *J. Micromech. Microeng.*, 2001, **11**, 257–262.
- 64 L. Brown, T. Koerner, J. H. Horton and R. D. Oleschuk, *Lab Chip*, 2006, **6**, 66–73.
- 65 K.-I. Min, T.-H. Lee, C. P. Park, Z.-Y. Wu, H. H. Girault, I. Ryu, T. Fukuyama, Y. Mukai and D.-P. Kim, *Angew. Chem., Int. Ed.*, 2010, **49**, 7063–7067.
- 66 J. Wang, W. Chen, J. Sun, C. Liu, Q. Yin, L. Zhang, Y. Xianyu, X. Shi, G. Hu and X. Jiang, *Lab Chip*, 2014, **14**, 1673–1677.
- 67 Z. Zhang, X. Wang, Y. Luo, S. He and L. Wang, *Talanta*, 2010, **81**, 1331–1338.
- 68 V. G. Kutchoukov, F. Laugere, W. van der Vlist, L. Pakula, Y. Garini and A. Bossche, *Sens. Actuators, A*, 2004, **114**, 521–527.
- 69 E. R. Murphy, J. R. Martinelli, N. Zaborenko, S. L. Buchwald and K. F. Jensen, *Angew. Chem., Int. Ed.*, 2007, **46**, 1734–1737.
- 70 H. Kim, H. J. Lee and D. P. Kim, *Angew. Chem., Int. Ed.*, 2015, **54**, 1877–1880.
- 71 S. Roesner and S. L. Buchwald, *Angew. Chem., Int. Ed.*, 2016, **55**, 10463–10467.
- 72 J. S. Lee, S. H. Lee, J. H. Kim and C. B. Park, *Lab Chip*, 2011, **11**, 2309–2311.
- 73 K.-I. Min, D. J. Im, H.-J. Lee and D.-P. Kim, *Lab Chip*, 2014, **14**, 3987–3992.
- 74 C. C. Lee, G. D. Sui, A. Elizarov, C. Y. J. Shu, Y. S. Shin, A. N. Dooley, J. Huang, A. Daridon, P. Wyatt, D. Stout, H. C. Kolb, O. N. Witte, N. Satyamurthy, J. R. Heath, M. E. Phelps, S. R. Quake and H. R. Tseng, *Science*, 2005, **310**, 1793–1796.
- 75 J. Kobayashi, Y. Mori, K. Okamoto, R. Akiyama, M. Ueno, T. Kitamori and S. Kobayashi, *Science*, 2004, **304**, 1305–1308.
- 76 S. Fornera, P. Kuhn, D. Lombardi, A. D. Schlueter, P. S. Dittrich and P. Walde, *ChemPlusChem*, 2012, **77**, 98–101.
- 77 A. M. Nightingale, T. W. Phillips, J. H. Bannock and J. C. de Mello, *Nat. Commun.*, 2014, **5**, 3777.
- 78 S. Duraiswamy and S. A. Khan, *Nano Lett.*, 2010, **10**, 3757–3763.
- 79 X. Yu, G. Cheng, M.-D. Zhou and S.-Y. Zheng, *Langmuir*, 2015, **31**, 3982–3992.
- 80 Q. Feng, J. Liu, X. Li, Q. Chen, J. Sun, X. Shi, B. Ding, H. Yu, Y. Li and X. Jiang, *Small*, 2017, **13**, 1603109.
- 81 L. Zhang, Q. Feng, J. Wang, S. Zhang, B. Ding, Y. Wei, M. Dong, J.-Y. Ryu, T.-Y. Yoon, X. Shi, J. Sun and X. Jiang, *ACS Nano*, 2015, **9**, 9912–9921.
- 82 C. P. Park, M. M. Van Wingerden, S.-Y. Han, D.-P. Kim and R. H. Grubbs, *Org. Lett.*, 2011, **13**, 2398–2401.
- 83 T. Noel and V. Hessel, *ChemSusChem*, 2013, **6**, 405–407.
- 84 A. Polyzos, M. O'Brien, T. P. Petersen, I. R. Baxendale and S. V. Ley, *Angew. Chem., Int. Ed.*, 2011, **50**, 1190–1193.
- 85 D.-H. Ko, W. Ren, J.-O. Kim, J. Wang, H. Wang, S. Sharma, M. Faustini and D.-P. Kim, *ACS Nano*, 2016, **10**, 1156–1162.
- 86 M. W. Bedore, N. Zaborenko, K. F. Jensen and T. F. Jamison, *Org. Process Res. Dev.*, 2010, **14**, 432–440.
- 87 E. M. Chan, R. A. Mathies and A. P. Alivisatos, *Nano Lett.*, 2003, **3**, 199–201.
- 88 M. Carboni, L. Capretto, D. Carugo, E. Stulz and X. Zhang, *J. Mater. Chem. C*, 2013, **1**, 7540–7546.

- 89 A. Knauer, A. Eisenhardt, S. Krischok and J. M. Koehler, *Nanoscale*, 2014, **6**, 5230–5238.
- 90 L. Wang, S. Ma, B. Yang, W. Cao and X. Han, *Chem. Eng. J.*, 2015, **268**, 102–108.
- 91 A. Nagaki, K. Imai, S. Ishiuchi and J.-i. Yoshida, *Angew. Chem., Int. Ed.*, 2015, **54**, 1914–1918.
- 92 Z. Yu, Y. Lv, C. Yu and W. Su, *Org. Process Res. Dev.*, 2013, **17**, 438–442.
- 93 I. Kreituss and J. W. Bode, *Nat. Chem.*, 2017, **9**, 446–452.
- 94 I. M. Mandity, S. B. Oetvoes and F. Fueloep, *ChemistryOpen*, 2015, **4**, 212–223.
- 95 H. Kim, A. Nagaki and J.-i. Yoshida, *Nat. Commun.*, 2011, **2**, 264.
- 96 M. W. Toepke, S. H. Brewer, D. M. Vu, K. D. Rector, J. E. Morgan, R. B. Gennis, P. J. A. Kenis and R. B. Dyer, *Anal. Chem.*, 2007, **79**, 122–128.
- 97 L. Zhang, J. S. Sun, Y. L. Wang, J. C. Wang, X. H. Shi and G. Q. Hu, *Anal. Chem.*, 2016, **88**, 7344–7351.
- 98 F. E. A. Van Waes, J. Drabowicz, A. Cukalovic and C. V. Stevens, *Green Chem.*, 2012, **14**, 2776–2779.
- 99 M. Movsisyan, E. I. Delbeke, J. K. Berton, C. Battilocchio, S. V. Ley and C. V. Stevens, *Chem. Soc. Rev.*, 2016, **45**, 4892–4928.
- 100 L. Vaccaro, D. Lanari, A. Marrocchi and G. Strappaveccia, *Green Chem.*, 2014, **16**, 3680–3704.
- 101 E. M. Chan, A. P. Alivisatos and R. A. Mathies, *J. Am. Chem. Soc.*, 2005, **127**, 13854–13861.
- 102 T. Fukuda, M. Sawada, T. Maki and K. Mae, *Chem. Eng. Technol.*, 2013, **36**, 968–974.
- 103 J. Haber, M. N. Kashid, N. Borhani, J. Thome, U. Krtschil, A. Renken and L. Kiwi-Minsker, *Chem. Eng. J.*, 2013, **214**, 97–105.
- 104 L. Kiwi-Minsker, M. Ruta, T. Eslanloo-Pereira and B. Bromley, *Chem. Eng. Process.*, 2010, **49**, 973–978.
- 105 K. Wang, Y. C. Lu, Y. Xia, H. W. Shao and G. S. Luo, *Chem. Eng. J.*, 2011, **169**, 290–298.
- 106 M. D. Bartlett, N. Kazem, M. J. Powell-Palm, X. Huang, W. Sun, J. A. Malen and C. Majidi, *Proc. Natl. Acad. Sci. U. S. A.*, 2017, **114**, 2143–2148.
- 107 N. Zaborenko, E. R. Murphy, J. G. Kralj and K. F. Jensen, *Ind. Eng. Chem. Res.*, 2010, **49**, 4132–4139.
- 108 B. Gutmann, D. Cantillo and C. O. Kappe, *Angew. Chem., Int. Ed.*, 2015, **54**, 6688–6728.
- 109 D. R. J. Acke and C. V. Stevens, *Green Chem.*, 2007, **9**, 386–390.
- 110 D. R. Reyes, D. Iossifidis, P. A. Auroux and A. Manz, *Anal. Chem.*, 2002, **74**, 2623–2636.
- 111 P. A. Auroux, D. Iossifidis, D. R. Reyes and A. Manz, *Anal. Chem.*, 2002, **74**, 2637–2652.
- 112 D. A. Horton, G. T. Bourne and M. L. Smythe, *Chem. Rev.*, 2003, **103**, 893–930.
- 113 N. K. Terrett, M. Gardner, D. W. Gordon, R. J. Kobylecki and J. Steele, *Tetrahedron*, 1995, **51**, 8135–8173.
- 114 Y. Zhao, Y. Cheng, L. Shang, J. Wang, Z. Xie and Z. Gu, *Small*, 2015, **11**, 151–174.
- 115 S. Mondal, E. Hegarty, C. Martin, S. K. Gokce, N. Ghorashian and A. Ben-Yakar, *Nat. Commun.*, 2016, **7**, 13023.
- 116 B. Swain, M. H. Hong, L. Kang, B. S. Kim, N.-H. Kim and C. G. Lee, *Chem. Eng. J.*, 2017, **308**, 311–321.
- 117 W. Y. Lin, Y. Wang, S. Wang and H. R. Tseng, *Nano Today*, 2009, **4**, 470–481.
- 118 H. F. Chan, S. Ma, J. Tian and K. W. Leong, *Nanoscale*, 2017, **9**, 3485–3495.
- 119 B. Zheng, L. S. Roach and R. F. Ismagilov, *J. Am. Chem. Soc.*, 2003, **125**, 11170–11171.
- 120 B. Hu, J. Li, L. Mou, Y. Liu, J. Deng, W. Qian, J. Sun, R. Cha and X. Jiang, *Lab Chip*, 2017, **17**, 2225–2234.
- 121 S. C. C. Shih, G. Goyal, P. W. Kim, N. Koutsoubelis, J. D. Keasling, P. D. Adams, N. J. Hillson and A. K. Singh, *ACS Synth. Biol.*, 2015, **4**, 1151–1164.
- 122 E. Garcia-Egido, V. Spikmans, S. Y. F. Wong and B. H. Warrington, *Lab Chip*, 2003, **3**, 73–76.
- 123 H. Zheng, W. Wang, X. Li, Z. Wang, L. Hood, C. Lausted and Z. Hu, *Lab Chip*, 2013, **13**, 3347–3350.
- 124 V. Georgi, L. Georgi, M. Blechert, M. Bergmeister, M. Zwanzig, D. A. Wuestenhagen, F. F. Bier, E. Jung and S. Kubick, *Lab Chip*, 2016, **16**, 269–281.
- 125 E. M. Chan, C. Xu, A. W. Mao, G. Han, J. S. Owen, B. E. Cohen and D. J. Milliron, *Nano Lett.*, 2010, **10**, 1874–1885.
- 126 N. Wang, F. Tan, Y. Zhao, C. C. Tsoi, X. Fan, W. Yu and X. Zhang, *Sci. Rep.*, 2016, **6**, 28928.
- 127 T. A. Meier, R. J. Beulig, E. Klinge, M. Fuss, S. Ohla and D. Belder, *Chem. Commun.*, 2015, **51**, 8588–8591.
- 128 J. Polte, R. Erler, A. F. Thuenemann, S. Sokolov, T. T. Ahner, K. Rademann, F. Emmerling and R. Krahnert, *ACS Nano*, 2010, **4**, 1076–1082.
- 129 A. Hoffmann, A. Kane, D. Nettels, D. E. Hertzog, P. Baumgaertel, J. Lengefeld, G. Reichardt, D. A. Horsley, R. Seckler, O. Bakajin and B. Schuler, *Proc. Natl. Acad. Sci. U. S. A.*, 2007, **104**, 105–110.
- 130 J. J. Heiland, R. Warias, C. Lotter, L. Mauritz, P. J. Fuchs, S. Ohla, K. Zeitler and D. Belder, *Lab Chip*, 2016, **17**, 76–81.
- 131 C. Lotter, E. Poehler, J. J. Heiland, L. Mauritz and D. Belder, *Lab Chip*, 2016, **16**, 4648–4652.
- 132 A. E. Kirby and A. R. Wheeler, *Lab Chip*, 2013, **13**, 2533–2540.
- 133 J. Heinemann, K. Deng, S. C. C. Shih, J. Gao, P. D. Adams, A. K. Singh and T. R. Northen, *Lab Chip*, 2017, **17**, 323–331.
- 134 E. Gross, X.-Z. Shu, S. Alayoglu, H. A. Bechtel, M. C. Martin, F. D. Toste and G. A. Somorjai, *J. Am. Chem. Soc.*, 2014, **136**, 3624–3629.
- 135 I. Lignos, R. Maceiczyk and A. J. deMello, *Acc. Chem. Res.*, 2017, **50**, 1248–1257.
- 136 J. P. McMullen, M. T. Stone, S. L. Buchwald and K. F. Jensen, *Angew. Chem., Int. Ed.*, 2010, **49**, 7076–7080.
- 137 P. J. Nieuwland, K. Koch, N. van Harskamp, R. Wehrens, J. C. M. van Hest and F. P. J. T. Rutjes, *Chem. – Asian J.*, 2010, **5**, 799–805.
- 138 W. Huyer and A. Neumaier, *ACM Trans. Math. Softw.*, 2008, **35**, 9.

- 139 J. E. Kreutz, A. Shukhaev, W. Du, S. Druskin, O. Daugulis and R. F. Ismagilov, *J. Am. Chem. Soc.*, 2010, **132**, 3128–3132.
- 140 S. Krishnadasan, R. J. C. Brown, A. J. deMello and J. C. deMello, *Lab Chip*, 2007, **7**, 1434–1441.
- 141 L. Gomez, V. Sebastian, S. Irusta, A. Ibarra, M. Arruebo and J. Santamaria, *Lab Chip*, 2014, **14**, 325–332.
- 142 J. N. Lee, C. Park and G. M. Whitesides, *Anal. Chem.*, 2003, **75**, 6544–6554.
- 143 K. Ren, Y. Chen and H. Wu, *Curr. Opin. Biotechnol.*, 2014, **25**, 78–85.
- 144 M. Saber, J. M. Commenge and L. Falk, *Chem. Eng. Sci.*, 2010, **65**, 372–379.